

RESEARCH

Open Access



Landslide Susceptibility Mapping of Urban Areas: Logistic Regression and Sensitivity Analysis applied to Quito, Ecuador

Fernando Puente-Sotomayor^{1,2*} , Ahmed Mustafa³  and Jacques Teller¹ 

Abstract

Although the Andean region is one of the most landslide-susceptible areas in the world, limited attention has been devoted to the topic in this context in terms of research, risk reduction practice, and urban policy. Based on the collection of landslides data of the Andean city of Quito, Ecuador, this article aims to explore the predictive power of a binary logistic regression model (LOGIT) to test secondary data and an official multicriteria evaluation model for landslide susceptibility in this urban area. Cell size resampling scenarios were explored as a parameter, as the inclusion of new “urban” factors. Furthermore, two types of sensitivity analysis (SA), univariate and Monte Carlo methods, were applied to improve the calibration of the LOGIT model. A Kolmogorov–Smirnov (K-S) test was included to measure the classification power of the models. Charts of the three SA methods helped to visualize the sensitivity of factors in the models. The Area Under the Curve (AUC) was a common metric for validation in this research. Among the ten factors included in the model to help explain landslide susceptibility in the context of Quito, results showed that population and street/road density, as novel “urban factors”, have relevant predicting power for landslide susceptibility in urban areas when adopting data standardization based on weights assigned by experts. The LOGIT was validated with an AUC of 0.79. Sensitivity analyses suggested that calibrations of the best-performance reference model would improve its AUC by up to 0.53%. Further experimentation regarding other methods of data pre-processing and a finer level of disaggregation of input data are suggested. In terms of policy design, the LOGIT model coefficient values suggest the need for a deep analysis of the impacts of urban features, such as population, road density, building footprint, and floor area, at a household scale, on the generation of landslide susceptibility in Andean cities such as Quito. This would help improve the zoning for landslide risk reduction, considering the safety, social and economic impacts that this practice may produce.

Keywords: Landslide susceptibility, Quito, LOGIT, Sensitivity analysis, Kolmogorov-Smirnov test, Andean cities, Urban factors

* Correspondence: fpuente@uce.edu.ec

¹Local Environmental Management and Analysis (LEMA), Urban and Environmental Engineering Dept., Liège University, Liège, Belgium

²Facultad de Arquitectura y Urbanismo, Universidad Central del Ecuador, Quito, Ecuador

Full list of author information is available at the end of the article



© The Author(s). 2021 **Open Access** This article is licensed under a Creative Commons Attribution 4.0 International License, which permits use, sharing, adaptation, distribution and reproduction in any medium or format, as long as you give appropriate credit to the original author(s) and the source, provide a link to the Creative Commons licence, and indicate if changes were made. The images or other third party material in this article are included in the article's Creative Commons licence, unless indicated otherwise in a credit line to the material. If material is not included in the article's Creative Commons licence and your intended use is not permitted by statutory regulation or exceeds the permitted use, you will need to obtain permission directly from the copyright holder. To view a copy of this licence, visit <http://creativecommons.org/licenses/by/4.0/>.

Introduction

Urban landslides in the Andes

The Andes is a sub-region located in western South America near the Pacific Ocean, named after the presence of the Andean mountains. The Andean mountain range is among the cordilleras with the highest elevations in the world and part of the Pacific Ring of Fire, a global mountain system characterized by frequent volcanic eruptions and earthquakes (Blanchard-Boehm 2004). The range crosses the territories of Colombia, Ecuador, Perú, Bolivia, Chile, and—with less significance for human settlements—Argentina and Venezuela. The Andes orography is of particular concern in terms of sustainable urban development because it has been subject to significant urbanization processes in recent decades, at an average of 20 m² per minute, particularly informal and diverse in typologies (Inostroza 2017). This growth includes metropolises such as Bogotá, Santiago, and Lima. Other medium-size cities, such as Medellín, Quito, and Cali, and smaller cities, also must be considered in terms of urban population growth. This urbanization has been induced by country–city migration and natural growth, for which housing and urban development—mostly informal and contributing to urban poverty—is a challenge to planning and management at all governmental levels, which have had to shift their policy paradigm (Blanchard-Boehm 2004; van Lindert 2016). Furthermore, cities are subject to urban risk in the Andes, where one of the most frequent risks, with high accumulated impact, is landslides.

Susceptibility analysis of landslide risk (LRisk) has been broadly studied in case studies at regional scales and mostly covering rural areas, often involving natural conditions and, to a lesser extent, considering anthropic factors, such as road networks and urban areas. However, urbanization is often treated only as a generic land-use category, without further detail. Against this background, LRisk is one of the main concerns for urban development in the Andes in light of physical and social factors. The geodynamics of this region make it prone to landslides. This condition is aggravated by climate change, in addition to the extreme events produced by El Niño climatic phenomena, which affect diverse locations of the region with an irregular time cycle. In some of these areas, urbanization has expanded rapidly in recent decades, as mentioned above. Cities in the Andes account for 70% of the population and the share of the urban population continues to grow rapidly. Unplanned urbanization is developing without any consideration of LRisks and governmental bodies have limited capacities to manage urban development (Comunidad Andina 2017; D'Ercole et al. 2009; UNISDR 2018). Evidence regarding landslide-prone conditions in the region has been presented by Kirschbaum and Stanley (2018) and

Sepúlveda and Petley (2015). These studies portray the concentration of landslide-susceptible areas in the irregular orography of Colombia, Ecuador, and Peru, with hundreds of fatalities. By comparison, fewer fatalities have occurred in neighboring countries in South America, with the exception of Brazil. Accordingly, disaster risk management (DRM) should be better integrated with land-use planning (LUP) for appropriate diagnostics and effective reduction of risks related to landslides.

Theoretical background

Key definitions

A landslide is defined as: “the downslope movement of soil, rock, and organic materials under the effects of gravity” (Highland and Bobrowsky 2008, p. 4). Its types include slides, falls, topples, flows, and lateral spreads, and combinations of these, whose causes can be geological, morphological, or anthropic (shaping of built or natural landscapes), which can be triggered by water, seismic, and volcanic activities (GEMMA 2007; USGS 2004). In complement, landslide disaster risk is the combination of natural hazard conditions, such as weak soil, intense precipitation, and earthquakes; vulnerability, such as soil cuts and fills, or structural weakness; and exposure, such as construction on LRisk-prone areas, as illustrated by Puente-Sotomayor et al. (2021).

This understanding of LRisk is directly related to landslide susceptibility, which beyond the definition of disaster risk as a social product, aims to identify the interaction between natural and built components, which is susceptible to landslides. By comparison, vulnerability—due to a closer relationship to anthropic action on land—can lead to analysis at minor scales. Anthropic vulnerability factors have less been taken into account in landslide susceptibility mapping (LSM); such in the case of road networks, specific urban land uses, and other human settlement features. The latter is a particular focus of attention for this study because extensive landslide disasters are produced in cities. However, few case studies address LSM in urban areas, such as reported by Bathrellos et al. (2009); Dragičević et al. (2014); Klimeš and Rios Escobar (2010); Lara et al. (2018); or, Lee, Baek, Jung, & Lee et al. (2020). Furthermore, of these, few consider vulnerability-related factors at a fine level, such as population, urban street networks, and urban structures (buildings), as noted in Table 1.

Reichenbach et al. (2018) define landslide susceptibility as the probability of incidence in a determined terrain relying on specific factors, including climate. These authors distinguish susceptibility from threat/hazard or vulnerability analyses in that the former is analyzed at a large scale and the data is acquired and processed at an aggregate level. Reichenbach et al. (2018) conclude from

Table 1 Review on landslide susceptibility modelling (LSM) modelling techniques, factors and inputs resolution used (Continued)

Reference code	Approach, Models, Techniques	Cell Size for resolution (m)	Year	Topography / DTM derivatives				Rainfall / Climate				Geology / Land Cover								
				Elevation / height /scarp	Slope angle / gradient	Slope aspect / sunlight exposition / orientation	Curvatures	Topographic Position Index (TPI)	Topographic Roughness Index (TRI)	Slope / Flow Direction	Other DTM derivatives	Annual Precipitation	Intense Precipitations	Long Precipitations	Potential rain effect (PRE)	Lithology / Geology	Geo (morpho) logical Units	Land Use / Vegetation Cover		
19 ^a	MCE, WLC	5	2010	✓											✓		✓			
20 ^a	WeF, MuF	20	2009	✓								✓					✓			
Total				12	20	16	9	9	3	2	2	3	6	8	2	0	1	14	2	14

Reference Geology / Land Cover
^aCorrespond to LSM studies in urban areas
^bThis modelling presented 35 factors; a summarized version of 13 is presented in this table
^cFor this classification, these factors have been grouped in the hydrology. However, they are also considered in the topography
^dOther DTM derivatives include: openness, side exposure index, hillshade, flow direction, and roughness
Notes:

- Diversity of factors for modelling have been classified by authors, criteria may vary
 - The selection of factors varies according to approaches. For instance, 7, 8, and 9 involve a wide range of topography-related factors
- References:**
 1. Gudiyangada Nachappa et al. (2020), 2. Psomiadis et al. (2020), 3. Lee, Baek, Jung, & Lee et al. (2020), 4. Wubalem (2020), 5. Chang et al. (2019), 6. Sitbu et al. (2019), 7. Meena et al. (2019), 8. Ramos-Bernal et al. (2019), 9. Pawluszek et al. (2018), 10. Lara et al. (2018), 11. Du et al. (2017), 12. Shahabi and Hashim (2015), 13. Feizizadeh and Blaschke (2014), 14. Dragičević et al. (2014), 15. Catani et al. (2013b), 16. Pascale et al. (2013), 17. Catani et al. (2013a), 18. Melchiorre et al. (2011), 19. Klimes and Rios Escobar (2010), 20. Bathrellos et al. (2009)
Abbreviations: AHP analytical hierarchical process, ANN artificial neural networks, CF certainty factor, DL deep learning, DTM digital terrain model, FFNN feed-forward neural network, FR data-driven frequency ratio, IV information value, JT jackknife test, LCVs landslide conditioning factors, LR logistic regression, LSI landslide susceptibility index, MCE multi-criteria evaluation, ML maximum likelihood, MuF multiple factor model, MURS mapping unit resolutions, NDWI normalized difference vegetation index, OB object based approaches, OWA ordered weighted average, PBA pixel based approaches, RF random forest, SA sensitivity analysis, SI susceptibility index, SVM support vector machine, WeF weight factor model, WLC weighted linear combination

Hydrology
 Roads
 Seismicity
 Anthropogenic, other

Table 1 Review on landslide susceptibility modelling (LSM) modelling techniques, factors and inputs resolution used (Continued)

Reference code	Geology / Land Cover		Roads		Hydrology		Seismicity			Anthropic, other		Random Value / other				
	Soils / textures	Normalized difference vegetation index (NDVI)	Potential erosion index (PEI)	Distance to roads	Road Density	Distance to drainage / streams	River / Gully Density	Flow Accumulation ^c	Topographic Wetness Index (TWI) ^c	Stream Power Index (SPI)	Distance to faults		Ground Peak Acceleration	Seismic Intensity / other Tectonic Features	Artificial Intervention / structures density	Declared flows
2				✓		✓					✓					
3 ^a	✓															
4	✓	✓				✓	✓									
5				✓		✓										
6						✓										
7			✓			✓					✓					
8			✓		✓									✓		
9																
10 ^a							✓								✓	
11				✓		✓					✓					
12	✓			✓		✓					✓					
13				✓		✓					✓					
14 ^a				✓		✓					✓					
15 ^b				✓		✓					✓					
16						✓					✓					
17						✓					✓					
18	✓			✓		✓					✓					
19 ^a																
20 ^a					✓											
Total	4	2	1	10	2	10	5	3	5	2	9	1	2	1	1	1

a global review of LSM that the usual determinant factors are slope, geology, and aspect; of these, the first two have a higher influence on the prediction power of models. They also state that results may vary according to methodologies, model validation, landslide types, triggering factors, and the researcher background. Other studies include precipitation, population density, and land use as significant factors (Hemasinghe et al. 2018; Sepúlveda and Petley 2015).

A brief review on LSM

Reichenbach et al. (2018) classify landslide susceptibility assessment into five groups, namely: (i) geomorphological mapping; (ii) analysis of landslide inventories; (iii) heuristic or index-based approaches; (iv) process-based methods; and (v) statistical modelling methods. The present work combines the heuristic approach officially adopted by the municipality of Quito as a preliminary input.

Modelling approaches A number of machine learning modelling techniques have been developed and applied in diverse locations globally to achieve the finest possible precision—each time with more sophistication—to provide better inputs into landslide risk reduction (LRR) policy and planning. Among the most used LSM techniques during the past two decades are multi-criteria evaluation (MCE), analytical hierarchical process (AHP), weighted linear combination (WLC), logistic regression (LR), data-driven frequency ratio (FR), random forest (RF), support vector machines (SVM), and artificial neural networks (ANN) (see Table 1). Most of the applied techniques have been proven to provide accurate results and differentiated advantages, sufficient for LSM practices and, therefore, LRR zoning policies. For instance, a comparison between LR, SVM, and RF applied to the Sihjhong watershed, Taiwan, found that RF performed best, whereas LR ran faster (Chang et al. 2019), which can be useful for large datasets, as in the present work. Regardless of the adopted method, research on LSM for Andean cities and regions is generally very limited and only a few application cases have been recently published (Puente-Sotomayor et al. 2021).

Modelling for LSM has prompted a discussion on the impact that different parameters of the process have on the accuracy of the produced results. In addition to the modelling technique used, these parameters include data preprocessing, scale or cell/pixel size of input factors, and the type and number of factors used for the modelling. Table 1 shows a brief comparison of the described parameters among previous studies.

Relevant LSM parameters Among the most relevant parameters is the preprocessing of data. There are different techniques to make factors comparable. These include different methods of normalization or standardization. Terminology varies. This study adopted the source assignation of weights in a discrete scale, also called weight-encoding, and data discretization using a percentile scale. Although standardization of weighted data for landslide susceptibility mapping is still an open discussion (Ronchetti et al. 2013), it is considered a valid option whenever intervals between ordinal categories are considered equal, regardless of statistical limitations such as the limited number of categories and overestimation of statistical power (Norman 2010; Pasta 2009; Williams 2019).

Regarding the factor parameters for an urban LSM, it must be noted that only five of the twenty reviewed studies relate to urban areas. However, even in these cases, the factors are similar to those applied in the other works, often covering regional scales and rarely involving cities, which the current work aims to analyze. Therefore, few previous studies include human/urban related factors, such as the buildings (see factors column in Table 1), population, and urban road networks, as applied to this work. It is relevant to note that, unless a specific factor approach or restraints on the availability of data are stated, the most considered factors are topography/digital terrain model (DTM) derivatives (primarily slope angle, aspect, elevation, and curvature), annual precipitation, geology (primarily lithology and land use/vegetation coverage), distance to roads, hydrology (primarily distance to drainage, density, and topographic wetness index (TWI), which also relates to topography) and distance to faults in the seismicity. Furthermore, beyond the possibility of including a large number of factors, this does not necessarily mean better performance of a model and the optimal number of factors in a LSM is still debatable (Catani, Lagomarsino, Segoni, & Tofani 2013a).

Another discussed parameter in the literature is the resolution at which the input data is set. Table 1 also includes this parameter for each revised work. Resolutions vary from 1 to 500 m cell sizes. Regardless of the restraints based on the availability, reliability of data, and the context itself, some studies have tested the sensitivity of this parameter with diverse approaches and results. For instance, Chang et al. (2019) concluded that the finest resolution of topographic data does not necessarily result in the best performance of a model. Regarding DTM derivatives, Pawluszek et al. (2018) found in an example case that the optimal resolution was 30 m, classified by SVM. Another case proved that the 50 m resolution contributed best to the performance of an RF technique (Catani et al. 2013b). Additional points of

view state that different land-surface factors also have different optimal scales, and that the applied modelling technique may also influence this parameterization. Therefore, multiscale approaches are recommended for better performance in complex terrain settings (Catani et al. 2013a; Sirbu et al. 2019). This has also been corroborated by Dragičević et al. (2014), who examined these types of complex and multi-scalar contexts from regional to municipal and local scales.

Once the data is pre-processed and made available for modelling, one common and simple theoretical model used is multi-criteria evaluation (MCE), which can be combined with sensitivity analysis, such as in Feizizadeh and Blaschke (2014) and Orán Cáceres et al. (2010), and explained below. A complementary approach to MCE is binary logistic regression (LOGIT), which is among the most used statistical methods for landslide susceptibility mapping (Reichenbach et al. 2018). This type of model helps to test weighted models, which do not support the assessment of the probability of landslide occurrences (Lombardo and Mai 2018). For this research, a LOGIT was applied, followed by an SA.

Sensitivity analysis

A further step in evaluating LOGIT models is to apply an SA (Reichenbach et al. 2018). SA is applied to determine the contribution of input parameters to the accuracy of the model prediction appraised in its outputs (Shahri et al. 2019; Poelmans and Van Rompaey 2010). The objective of sensitivity analysis is to help adjust the calibration of the studied parameters involved in the LSM model to improve its predicting/classification power. Among different methodologies, two stand out: the simple, univariate, or “one-at-a-time” (OAT) method, and the stochastic/random-selection method, also called “Monte Carlo”, whose applications vary according to the needs of the field of practice (Bouyer 2009). Details of both methods are explained in the methods and results sections.

Methods

Study area and its landslide risk-reduction policy background

Quito, the capital of Ecuador, is the most populated of two existing metropolitan districts (regions) in the country, with 2,781,641 inhabitants projected for 2020 (INEC 2016). The jurisdiction of the Metropolitan District of Quito (DMQ) covers 4235.2 km², of which 10% is urban land with 286,412 housing units (Quito Municipio del Distrito Metropolitano 2015). As one of the Andean mountain cities, Quito has suffered from multiple natural threats, including landslides, volcano eruptions, floods, and earthquakes. Hence, exposure to risks has been further exacerbated, given the fast population growth and the uncontrolled urbanization process.

Accordingly, Quito has collected geodata relating to landslide disaster events during the past two decades. This has strengthened the city’s management capacities and its approach to preventive policies and actions (Rebotier 2016), in addition to preparedness and response. Most recently, resiliency has been adopted as an urban policy, to the point of being institutionalized, with the creation of a Resiliency Department and the design of the city’s resiliency strategy (Quito Alcaldia del Distrito Metropolitano 2018; Quito Municipio del Distrito Metropolitano 2017).

Landslide risk reduction (LRR) policies in Quito have a history of approximately one decade. They began with landslide-related land-use zoning as part of the local plan, in 2011 (Puente-Sotomayor et al. 2018). Previously, building regulations included generic risk prevention measures, such as setbacks from ravines, slope borders, and rivers (Concejo del Distrito Metropolitano de Quito 2003). For lahar-prone areas, a transfer of responsibility from government to users was used, applying a notarized responsibility to the owner for building on high-risk areas, prior to city approval (Concejo del Distrito Metropolitano de Quito 2011). Since 2014, this has no longer been allowed in national laws, which assign criminal liability of the generated risks to any official that approves subdivisions or projects in risk zones (Ecuador Asamblea Nacional 2014).

During the past decade, the landslide preventive/reductive approach was materialized by establishing the LRisk zone (ZR) category in the local LUP. Construction was strictly banned in ZR areas. This zoning policy intuitively and imprecisely combined slopes (at the 1:5000 scale), soil stability (at the 1:25,000 scale), and field inspections as the only inputs in 2011. The application of this regulation triggered around 40 complaints per year from users, who claimed they were affected socially, through the violation of their housing rights; and, economically, due to previous investments and rent expectations related to the property labeled at-risk. In 2013, a reform to this ordinance relaxed the policy by returning to owners the right to build on ZRs, who provided geotechnical studies that justified their projects. This revealed limitations of the technical capacity of users and officials, and the problem with defining “mitigation”, which subsequently evidenced the poor accessibility to geotechnical risk relief for low socio-economic strata. A new reform in 2015 cancelled the ZR land-use category and converted it to an overlay map, which, in practice, did not change the policy (Puente-Sotomayor et al. 2018). By 2015, the first landslide susceptibility studies were produced. The outputs of these studies were expected to improve the ZR policy. However, they have not yet been articulated with the LUP. These studies’ outputs have been labeled as official data and were used as part of the input data for this research.

A brief comparison between the ZR layer, for which the limits have not yet changed, the existing landslide susceptibility study (FUNEPSA et al. 2015), and a landslide events database from 2005 to 2017 (see Fig. 1), provided by the Metropolitan Emergency Operations Committee of Quito (COE-M), reveals inconsistencies between the policy, research, and facts.

Only 8% of recorded landslide events are contained in ZR polygons, 25% of ZR do not match with the high and very-high susceptibility areas, and 81% of high and very-high susceptibility areas are not covered by the ZR polygons. This presumably means that vast areas should be considered as landslide-prone, while other areas, although smaller in proportion, probably

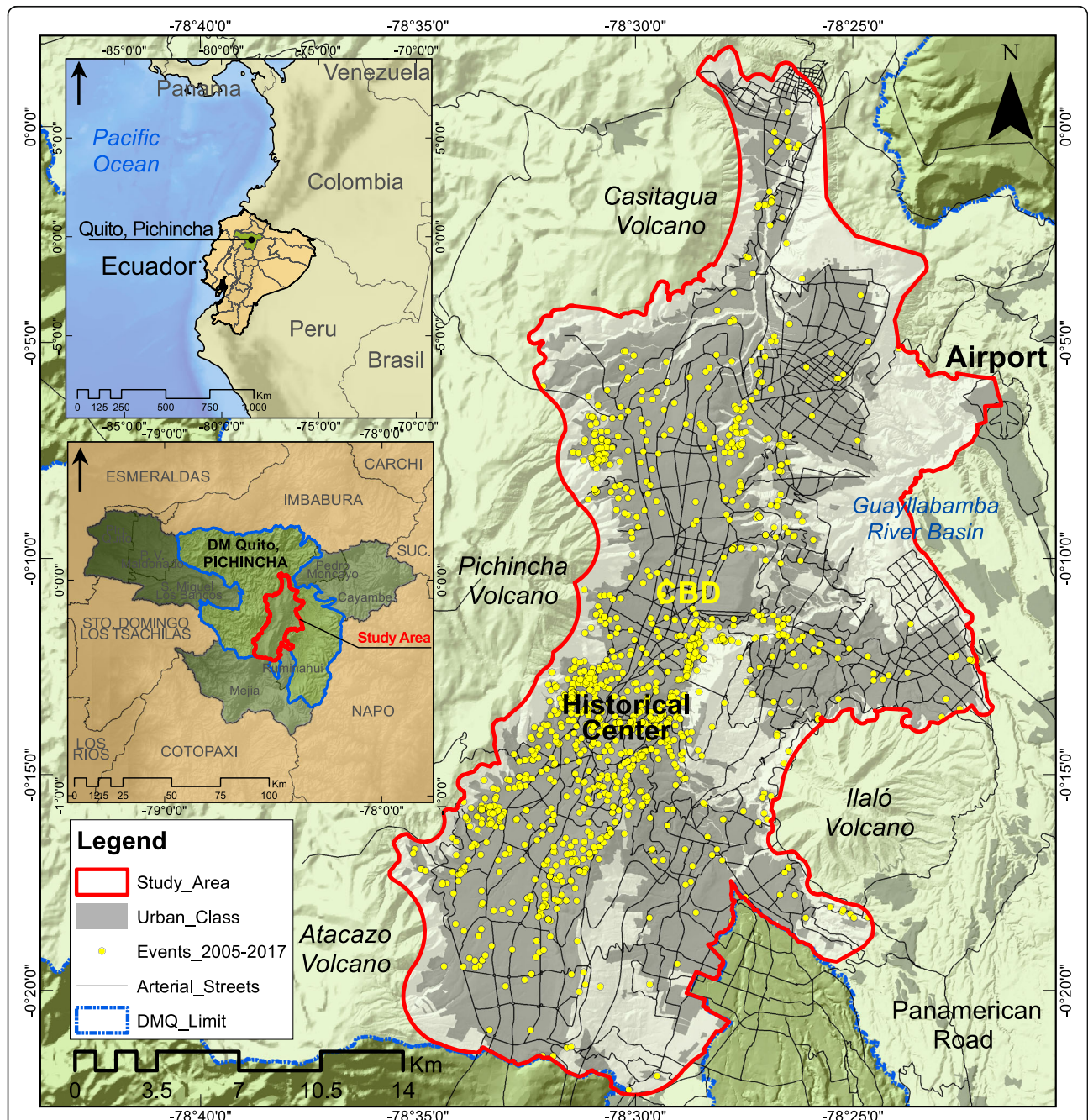


Fig. 1 Study Area in the Metropolitan District of Quito, displaying the 2005–2017 period landslide events. Data Source: MDMQ, IGM Ecuador. Legend: Study Area (red line), Urban Class (gray polygon), Landslide Events during the 2005–2017 period (yellow dots), Arterial Streets network (black continuous lines) and the Metropolitan District of Quito jurisdictional limit (dashed blue line)

do not need a protection policy (Puente-Sotomayor et al. 2018).

Purpose, objectives and scope

The main purpose of this study was to produce a reliable Landslide Susceptibility Map (LSM) that can support LRR policies for urban Quito (see study area section). This represents a progress from previous actions regarding landslide preventive/reductive zoning in this city. For this purpose, specific objectives included the examination of the incidence of urban-related factors in LRisk susceptibility; providing quality inputs for better ZR delimitation, considering the implications for safety, housing rights, and the economy; and generating improvements, further discussion and action in the local LSM processes, by exploring different parameters such as modelling approaches, scale, data generation, and factors selection.

The practical scope of this study was to derive a landslide susceptibility map based on a binary logistic regression model combined with a sensitivity analysis (SA) to provide optimal calibration options for factor coefficients used in the model. Developing an evidence-based LSM that considers SA is an indispensable input for developing an urban policy backed by a socio-political consensus (Orán Cáceres et al. 2010). The context of application will be the urban core of the DMQ, including its surrounding peri-urbanized areas, as described below.

This research is built upon data collected during a LRisk analysis produced by the municipality in 2015. This study delivered a weighted multi-criteria theoretical model including six factors that were surveyed and processed. These factors are slope, intense precipitations, soil stability after former large landslides, lithology, land use/vegetation coverage, and seismic intensity. Each factor had partial weights/susceptibilities proposed by local experts in the fields of geotechnics, meteorology, geography, disaster management, and seismology. The results of this model portrayed a landslide susceptibility map for Quito and its satellite “conurbated” areas (an approximate total area of 610 km²) using the map algebra GIS tool to sum the partial weights as shown in Fig. 2 (FUNEPSA et al. 2015).

Inputs and preprocessing

Initially, our study proposed to develop a binary logistic regression model on the basis of six factors identified by the municipality experts, plus other related to the Quito urban settings, which we aimed to experiment with. A dataset of landslide events that occurred from 2005 to 2017 was therefore collected from the COEM of Quito. This database includes around 1400 events, including rotational and translational

landslides, flows, and topples, all considered generically as landslides (USGS 2004). A minor limitation is that the dataset suffers from some underreporting, and unbalanced and unstructured elements.

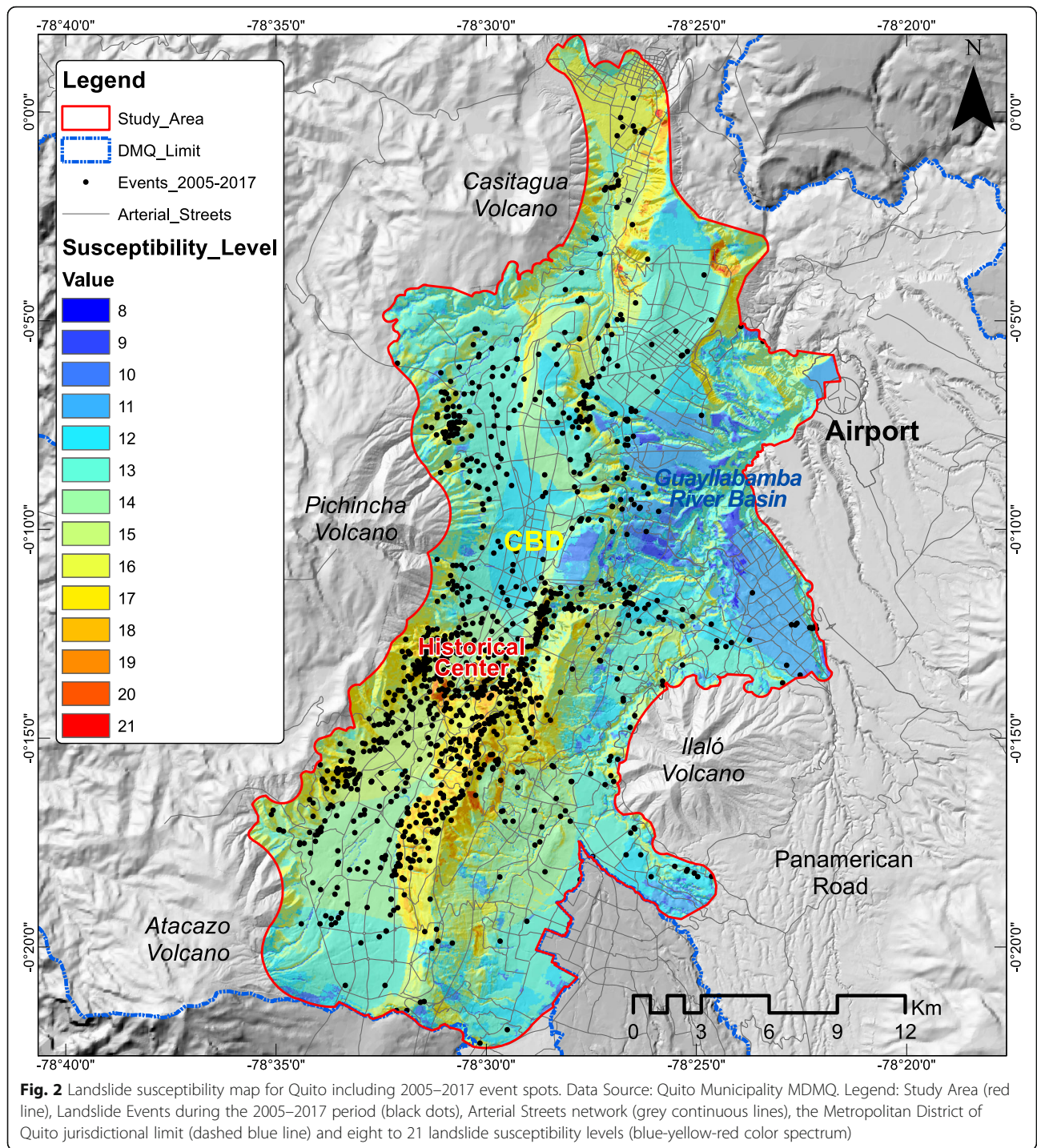
From the data of the six initial factors, the first LOGIT was applied. Then, four additional factors were included in two steps to test the model. As a first addition, population, provided by the National Institute of Statistics and Census (INEC), and floor area, provided by the Quito municipality (MDMQ), were included to construct a second LOGIT. Then, road density and building footprint area, also provided by the MDMQ, were added to run the final LOGIT. All four additional factors were pre-processed and adapted for this research work. As explained in the introduction section, considering the urban context of Quito, where all of the landslide events were registered, this research aimed to determine the incidence of these factors on the results, whose content was more relevant to the urban context, i.e., buildings, streets, and population. Details of all of the ten factors included in this study are provided in Table 2.

Resolution

The dependent factor, landslide events (binary), and the ten independent, explanatory factors were pre-processed in raster files, with a cell size (disaggregation level) of 50 m. This was the resolution at which the lithology, land coverage, seismicity, precipitations, soil stability, and slope were previously provided by the municipality surveyors. Complementarily, the additional four “urban” factors were converted from a scale at which the detail of buildings, blocks, and streets was legible (1:1000 approximately), which was logically consistent with the 50 m cell size of the other six factors. Therefore, all of the datasets were standardized to this resolution. In this regard, the theoretical background review implied that, although scale may determine the modelling performance, performance is also dependent on the context and complexity of the process. For this study, although the secondary source input data was pre-processed at a 50 m cell size, an aggregation process through resampling GIS techniques (nearest neighbor mode) were applied to suit the complete datasets at resolutions of 100, 200, and 500 m before the application of the LR modelling for each resolution. Subsequently, the results provide a rationale to retain the original scale.

Standardization

To manage a standard scale of factor values before applying the LOGIT, the following process was undertaken. The binary layer of landslide events records one of two categories for each area unit or cell: true (or one), when one or more landslide events occurred in it; or, false (or zero), when no landslides occurred in it. Two



standardization types proceeded. The first six factors provided by the municipality were previously converted from either classified continuous data or categorical data to weights in a discrete 1-to-4 scale. The additional four factors, all continuous, were classified using natural breaks in four classes, to correspond to the 1-to-4 scale. The details of this conversion are shown in Table 3. The complementary data, i.e., the additional four factors that

were collected in vector format, were then converted into raster TIFFs to fit with the remainder of the dataset (initial six factors).

By looking at the data categories and their assigned weights, the contribution from the local experts in generating the datasets is notable. This can be seen, in particular, for factors such as lithology, land-use/vegetation coverage, and stability, whose information is specifically

Table 2 Input data for landslide susceptibility mapping in Quito

Code	Content	Disaggregation level	Specifications, type	Data Source	Year
bin	<i>Landslide Events</i>	Point	Binary	COE-M Quito	2005–2017
1geo	<i>Lithology</i>	50 m	Pre-discretized from categorical to weights (weighted classes)	FUNEPSA et al. 2015	2015
2cov	<i>Land Use/Vegetation Cover</i>	50 m	Pre-discretized from categorical to weights	FUNEPSA et al. 2015	2015
3sei	<i>Seismicity</i>	50 m	Pre-discretized from categorical to weights	FUNEPSA et al. 2015	2015
4pre	<i>Intense Precipitations (in 24 h)</i>	50 m	Pre-discretized from continuous to weights	FUNEPSA et al. 2015	2015
5sta	<i>Soil Stability (from former landslides)</i>	50 m	Pre-discretized from categorical to weights	FUNEPSA et al. 2015	2015
6slo	<i>Slope</i>	50 m	Pre-discretized from continuous to weights	FUNEPSA et al. 2015	2015
7pop	<i>Population</i>	Block Scale	Continuous, discretized by natural breaks to weights	INEC	2010
8roa	<i>Streets (Roads) Density</i>	Street segment	Continuous, discretized by natural breaks to weights	STHV – MDMQ	2016
9bui	<i>Floor Area</i>	Building Scale	Continuous, discretized by natural breaks to weights	STHV – MDMQ	2017
10gro	<i>Building Footprint Area</i>	Building Scale	Continuous, discretized by natural breaks to weights	STHV – MDMQ	2017

NOTE: COE-M is the Metropolitan Emergency Operations Committee of Quito, FUNEPSA et al., (2015) is the report containing the official surveyed data for Quito Municipality - Disaster Risk Management Division, INEC is the Ecuadorian National Institute of Statistics and Census, STHV-MDMQ is the Secretariat of Territory, Habitat and Housing of Quito Municipality

related to the Quito context. Furthermore, It is important to mention that, for the case of the slope factor, the class “greater than 50°” is weighted as 3 and not 4, as one would suppose. This is due to the fact that most of the local geology type, the “cangahua”, found at this slope range and in most of the study area, is less susceptible to landslides than flatter slope ranges and has reported much less events, according to the local data mining experts. Regarding the rainfall, the meteorology surveyors stated that the Quito region is not affected by long-term persistent rainfall, which triggers landslides in other parts of the world, such as Central America or Southeast Asia, or in territories affected by El Niño phenomena extreme events, which are not regular in terms of time cycles and occur every 25 or 30 years. Instead, in Quito, landslides are more likely triggered by intense precipitations, which is why this variable was included instead of other climate-related factors, such as annual precipitation rates. Inclusive, long precipitation was not considered in the reviewed scientific articles, as shown in Table 1.

A second standardization process for the ten explanatory factors was applied and tested. It was based on a percentile discretization. The aim of applying percentile discretization was to have a finer value than the 1-to-4 scale. This also helped to correct a distortion existing in the provided data, produced by a marginal portion of outliers that widened the absolute value range of the dataset, which is an advantage of this discretization method (Grzenda 2020). This distortion occurred

particularly with the data of the floor area and building footprint area. Table 4 shows how the ten factors were discretized through percentiles. The categorical data weights were assigned to their corresponding percentile of the 1-to-100 scale, considering in it three equal segments (assuming intervals between weights as equal units in a discrete scale). For the remaining continuous data factors, the new values were simply the corresponding percentile.

Logistic regression

Following the preparation of the data, the LOGIT proceeded. In regard to the sampling method, two sets of elements (the binary sample of cells) with equal number of items were then selected to test the LOGIT. The first set had cells that registered the occurrence of landslides (an average of 1.29 events per cell), in total, 1139 cells with a true/one value. The second set had cells that did not register landslides, i.e., false/zero value. Considering the 1139 true values, an equal number of false value cells were randomly chosen from more than 222,000 remaining equivalent value cells in the study area.

A generalized linear model regression function in the programming platform (MATLAB_R2018b) was then applied to obtain the values of the coefficients for all ten factors and the intercept of the function. With these values, the logistic regression (Eq. 1) was applied to obtain the landslide susceptibility values for all cells for the study area. These values provide the probability of occurrence of a landslide, varying from 0 (null probability)

Table 3 Conversion of factor classes or categories to weights (weights encoding) of input factors for LSM for Quito. Source: MDMMQ, INEC, adapted by authors

Code	Weights (Partial Susceptibilities):	1	2	3	4
1geo	Slope (degrees):	<ul style="list-style-type: none"> • 0° - 10° 	<ul style="list-style-type: none"> • 10.1° - 25° 	<ul style="list-style-type: none"> • 25.1° - 35° • > 50° 	<ul style="list-style-type: none"> • 35.1° - 50°
2cov	Lithology (categories):	<ul style="list-style-type: none"> • Cotopaxi Lahars: steep ledges and slopes. Slopes and canyons or deep throats of ravines and rivers • Pululahua Domes: fractured dacites from the volcano, but they appear compact and with resistant weathering 	<ul style="list-style-type: none"> • Quito Lake Deposits • Colluvial Mass Movements • Colluvial Conglomerates • Colluvials • Casitagua Volcanics • Undifferentiated Volcanic Lahars • Pichincha Volcanics • Cangahua formations: compacted ashes, pyroclastic; lava 	<ul style="list-style-type: none"> • Cangahua formations: undifferentiated ashes-lapillistone with destroyed surfaces, strongly bisected in hills with rounded tips 	<ul style="list-style-type: none"> • Alluvial terraces • Pululahua pyroclastic flows • Guayllabamba, San Miguel and Pisque Formations: sequences of volcanic sands, pyroclastic flows, silts, lahars; at the base: fluvial-lake sequence, occasionally very crumbly
3sei	Land Use / Vegetation Cover (categories):	<ul style="list-style-type: none"> • North Andes mountain bushes • Always-green North Andean high-mountain forests • Mountain pasture • High-mountain and mountain-moor grassland 	<ul style="list-style-type: none"> • Reservoirs • Inter-Andean dry bushes • Inter-Andean dry forest • Eucalyptus forests • River vegetation from xerophytic mountain floor • Inter-Andean mountain Saxi-cola Vegetation 	<ul style="list-style-type: none"> • Airport • Short-cycle crops • Cropped grass • Natural grass 	<ul style="list-style-type: none"> • Quarries • Buildings • Eroded soils
4pre	Soil Stability (categories):	<ul style="list-style-type: none"> • Stabilized 	<ul style="list-style-type: none"> • Latent 	<ul style="list-style-type: none"> • Reactivated • Colluvial 	<ul style="list-style-type: none"> • Active
5sta	Intense Precipitations in 24 h (stations types: a. <i>maximum</i> (mm) / $n > 10$. <i>Rt</i> = 100 years, b. Average rain (mm) / $n < 10$ years):	<ul style="list-style-type: none"> • < 75.4 (a) • < 50 (b) 	<ul style="list-style-type: none"> • 76.4–91.88 (a) • 51–90 (b) 	<ul style="list-style-type: none"> • 91.88–107.34 (a) • 91–130 (b) 	<ul style="list-style-type: none"> • 107.34–122.79 (a) • 137–175 (b)
6slo	Seismic Intensity (European Macro-seismic Scale, ordinal):	Not applicable	<ul style="list-style-type: none"> • EMS VII 	<ul style="list-style-type: none"> • EMS VIII 	Not applicable
7pop	Population (Inhabitants):	<ul style="list-style-type: none"> • 0–1.81 	<ul style="list-style-type: none"> • 1.82–5.56 	<ul style="list-style-type: none"> • 5.57–12.47 	<ul style="list-style-type: none"> • 12.48–31.86
8roa	Road Density (m/Ha):	<ul style="list-style-type: none"> • 0–7.50 	<ul style="list-style-type: none"> • 7.51–18.16 	<ul style="list-style-type: none"> • 18.17–31.99 	<ul style="list-style-type: none"> • 32–100.70
9bui	Floor Area (m ²):	<ul style="list-style-type: none"> • 0–4,180.33 	<ul style="list-style-type: none"> • 4,180.34–35,950.76 	<ul style="list-style-type: none"> • 35,950.77 – 104,508.01 	<ul style="list-style-type: none"> • 104,508.02–213,196.34
10gro	Building Footprint Area (m ²):	<ul style="list-style-type: none"> • 0–3,344.26 	<ul style="list-style-type: none"> • 3,344.27–34,278.63 	<ul style="list-style-type: none"> • 34,278.64 – 104,508.01 	<ul style="list-style-type: none"> • 104,508.02–213,196.34

NOTE: The data collected for intense precipitations was standardized by assigning partial susceptibilities (weights) to data provided by two types of meteorological stations: a. those with records of more than 10 years; and, b. those with records of less than 10 years. For the meteorology notation consider: *n* period in years, *Rt* return time. Further details on the calculation to complete the intense precipitations dataset are available in the FUNEPSA et al. report (2015)

Table 4 Conversion table of categorical data from weights encoding to percentile discretization, and continuous data to percentiles

Categorical Data Factors:	<ul style="list-style-type: none"> • <i>Lithology</i> • <i>Land Use/Vegetation Coverage</i> • <i>Seismic intensities</i> • <i>Intense Precipitations</i> • <i>Soil Stability</i> after former landslide events 	Weights (Partial Susceptibilities) ^a :	1	2	3	4
		Percentile Values:	1	33	67	100
Continuous Data Factors:	<ul style="list-style-type: none"> • <i>Slope</i> • <i>Population</i> • <i>Road Density</i> • <i>Floor Area</i> • <i>Building Footprint Area</i> 	Weights (Partial Susceptibilities) ^b:	1	2	3	4
		Percentile Values:	Corresponding percentile (from 1 to 100)			

^aAssigned according to FUNEPSA et al. (2015)

^bClassified by natural breaks, except for *slope*, classified according to FUNEPSA et al. (2015)

to 1 (absolute occurrence). These values helped generate the reference landslide susceptibility map. This process was first undertaken for the six initial factors; second, with the addition of *population* and *floor area* as new factors; and finally, with the addition of *road density* and *building footprint area*. The area under the receiving operating characteristic (ROC) curve (AUC) was the performance indicator chosen for the LOGIT model, considering it is common in evaluation of the prediction accuracy of models for natural hazards (Shahri et al. 2019; Wang et al. 2020).

Equation 1 Logistic regression function for landslide susceptibility mapping

$$ls = \frac{1}{1 + e^{-(b_0 + b_1x_1 + b_2x_2 + \dots + b_nx_n)}}$$

where:

ls = landslide susceptibility: the probability of occurrence of a landslide (between 0 and 1)

e = the mathematical constant e (2.71828)

b₀ = the intercept of the logistic function

b_n = the coefficient of factor x_n

x_n = the factor number n

Sensitivity Analysis – univariate method

After the generation of a referential susceptibility map and the validation of the LOGIT model that generated it using the AUC/ROC value, SA was performed to test the sensitivity of the model outputs to changes in one, many, or all selected parameters. For this research, the selected referential metric was the AUC value as the output for all of the generated simulations, as applied to SA by Poelmans and Van Rompaey (2010). Sensitivity analyses were performed using two methods.

The first was the simple, univariate, or OAT method, which is simple to apply and assess. It consisted in changing one “free” parameter of the model at a time to generate variations of the model, within a defined range and with a defined interval for the changes. In this case, while one factor changes its coefficient, the others remain unaffected (fixed parameters) and remain as the

references. For the model used in this research, the parameters changed were each of the ten coefficients generated by the LOGIT model. A set of multipliers ranging from 0.1 to 20 with an interval of 0.1 modified each of the coefficients of the ten factors, one at a time, to generate a total of 2000 susceptibility maps, from which AUC values (outputs) were generated and plotted. The AUC values higher than the reference AUC value (the first generated) indicates that their corresponding models are better calibrated than the reference. This was reproduced for the weights-encoded and the percentile-discretized models.

Kolmogorov–Smirnov test for sensitivity

A two-sample Kolmogorov–Smirnov (K-S) test was applied to the univariate test results for both weights and percentile-based discretization methods as another means to determine the sensitivity of the factors. As a metric, the D-statistic (also called the KS-statistic) values are provided, indicating the D-critical value, as calculated using Eq. 2. These provide a more insightful picture than the p-values of the same test, which considered an alpha value of 0.05 and were also calculated. The K-S tests were tabulated using the empirical distribution functions of two samples—ones and zeros—from each resulting map derived from the changes of the simple/univariate method, i.e., the distribution of the cell values corresponding to event occurrence cells (1139 observations/elements) compared to a distribution of a randomly selected similar number of non-occurrence cells. This test was applied only to the results of the simple sensitivity analysis due to limitations in computer processing capacities and simplicity of visualization in charts, which provided for better communication of results.

Equation 2 Calculation of the D-critical value for a two-sample K-S test

$$D_\alpha = c(\alpha) \sqrt{\frac{n_1 + n_2}{n_1 n_2}}$$

where:

$D\alpha$ = D-critical value of the K-S test at an alpha value α

α = Alpha value determined for the K-S test (0.05 for this case)

$c(\alpha)$ = constant based on α (1.36 for this case)

n_1 = first sample size (1139 for this case)

n_2 = second sample size (1139 for this case)

Sensitivity Analysis—Monte Carlo method

A second method to test the sensitivity based on factors used random variations for all of the factors, from one to all at a time, also within a defined range and with a defined interval. This is also called the Monte Carlo or stochastic method. For this research, multipliers of one or more coefficients at a time ranged from 0.1 to 5 with an interval of 0.1. The number of simulations for this random selection of possibilities was set to 8000, which may vary in replications of this study, according to the computer’s processing capacities. Once again, AUC values (outputs) were generated and those higher than the reference AUC value indicated that their corresponding models with their modified coefficients’ values had a better performance calibration than the reference itself (Bouyer 2009). To better illustrate this, a table of random simulation calibrations is provided in the results, plus a chart showing the two best predictor factors.

Methodology summary and software used

To summarize, Table 5 shows all of the methodology and specific tools applied for this research.

Regarding the software packages used to process data for this research work, GIS software (ArcMap 10.3) was applied to produce all maps using the integration, transformation, and geoprocessing tools, and conversion of shapefiles into raster TIFF files to make them suitable for calculation for the LOGIT model and the SA. A programming platform for matrix analysis (MATLAB_R2018b) was used for the SA, for which, particularly the

generalized linear model regression, (glmfit function) and the AUC value computation (perfcurve function), were applied. For the two-sample K-S test, the function used was kstest2. The subsequent outputs were TIFF files for mapping and CSV datasets to produce graphs and charts in a spreadsheet package (Microsoft Excel) and a presentation/illustration package (Microsoft PowerPoint). Tables were adjusted to a word processing package (Microsoft Word) format. The input TIFF files and the programming platform (MATLAB_R2018b) code are provided as [Supplementary Material](#) to this research work

Results

LOGIT results by adding urban factors and a standardization variant

The first results portray the changes regarding the addition of factors, departing from the six-factor initial LOGIT model, which corresponds to the map shown in Fig. 2, which delivered weight scores from eight (lowest landslide susceptibility) to 21 (highest landslide susceptibility). This considered six factors: *lithology, land use/vegetation coverage, seismic intensities, intense precipitations, soil stability after large events, and slope*. Subsequently, the LOGIT was tested with eight factors and finally with 10 factors. The eight-factor model included two more factors: *population* and *floor area*, while retaining the weights encoding (continuous factors classified by natural breaks). The 10-factor model included two more factors: *road density* and *building footprint area*, also weights-encoded. As new factors were added, the coefficients with the highest values changed their relative descending order (from highest to lowest value). For the 10-factor model, a variation by percentile-discretization of factor values was applied, which delivered a fourth set of results. The four models’ results, including their corresponding AUC value, can be seen in Table 6. The initial multi-criteria evaluation (MCE) official map and the 6, 8, and 10-factor reference maps

Table 5 Methodology summary and applied tools

	<u>6-Factor Model</u>	<u>8-Factor Model</u>	<u>10-Factor Model</u>	
	<u>Weights-encoding</u>	<u>Weights-encoding</u>	<u>Weights-encoding</u>	<u>Percentile-discretization</u>
LOGIT with referential landslide susceptibility map and AUC value	✓	✓	✓	✓
Resolution tests of 50, 100, 200 and 500 m cell size, through LOGIT and AUC value			✓	
Sensitivity Analysis – Univariate method, variations plot and AUC values higher than reference			✓	✓
K-S test			✓	✓
Sensitivity Analysis – Monte Carlo Method, visualization of 2 best predictors and AUC values higher than reference			✓	✓

Table 6 Output values from LOGIT modelling for landslide susceptibility in Quito

Code	Factor	6-Factor Model		8-Factor Model		10-Factor Model		Percentile discretization	
		Weights encoding		Weights encoding		Weights encoding		Percentile discretization	
		Coefficient (β value)	Descending Order	Coefficient (β value)	Descending Order	Coefficient (β value)	Descending Order	Coefficient (β value)	Descending Order
0int	Intercept	-0.5281		-10.7830		-4.1375		-2.4317	
1geo	Lithology	0.3756	3	0.2550	5	0.1905	5	0.0160	2
2cov	Land use/vegetation coverage	0.8483	1	0.4250	4	0.0125	7	0.0122	3
3sei	Seismic Intensity	-0.1628	6	-0.0910	7	-0.2004	9	-0.0110	10
4pre	Intense Precipitations	0.6528	2	0.4500	2	0.3943	3	0.0238	1
5sta	Stability after large events	0.0247	5	0.1160	6	-0.1526	8	0.0047	5
6slo	Slope	0.3756	4	0.4450	3	0.3896	4	-0.00045	7
7pop	Population	-	-	0.6840	1	0.5348	2	0.0034	6
8roa	Road Density	-	-	-	-	0.6101	1	0.0052	4
9bui	Floor Area	-	-	-0.1280	8	0.0566	6	-0.0040	9
10gro	Building Footprint Area	-	-	-	-	-0.2364	10	-0.0038	8
	AUC value	0.755		0.784		0.7928		0.7417	

NOTE: Descending Order columns refer to the relative order position that explanatory factor coefficients have among their group in the model by sorting them from the highest to the lowest value

(weights and percentile standardizations), can be seen in Fig. 3. The last two maps (d and e) in this figure were used for SA.

Results based on resolution inputs

A previous approach in addition to testing SA based on factors, was to consider the impact of the variation in the input data cell size on the final result, using the AUC value as a metric of validation. To test this sensitivity, the minimum resolution (50 m) provided by the sources as input data was resampled to 100, 200, and 500 m. The selected standardization method for this test was the weighed-encoding approach because it performed with a higher AUC value than the percentile-discretized model (see Table 6). To illustrate changes based on resolution inputs, Table 7 shows the descriptive statistics of AUC values after simulating 100 LSM units for each of the cited cell sizes. It can be noted that the highest average AUC value corresponds to the 500 m cell case. Nonetheless, the model corresponding to this cell size is the least stable, as indicated by its standard deviation and range, which are higher than the cases of the other cell sizes. In contrast, the original 50 m cell size provided more stable behavior while maintaining a reasonable and reliable AUC value before testing other parameters for SA.

Univariate SA results

With the ten-factor model, executed by both standardization methods (weights and percentiles), an SA based on factors was performed. For the weights-encoding method, the univariate SA produced susceptibility maps

whose AUC values (the metric of the sensitivity) were plotted, as seen in Fig. 4. From this analysis, and from the range and interval set to produce the coefficient variations, there were 241 AUC values higher than the reference AUC value (0.7928) out of 2000 simulations. When observing this chart, the AUC improvement is slightly higher than the reference. From the 2000 simulations, the highest AUC value was 0.7943, which is almost 0.2% higher than the reference. The coefficients that had the strongest impacts on the results, when the variations were applied, belong to the *population*, *slope*, and *road density* factors.

The same test was applied to the percentile-discretized case. The results delivered 34 AUC values higher than the reference AUC value (0.7417) out of 2000 programmed simulations. The maximum improvement reached an AUC value of 0.7419 with a marginal improvement of 0.03%. The plotting of all AUC values derived from this univariate method variations' susceptibility maps/datasets can be seen in Fig. 5. *Precipitations*, *land-use cover*, and *road density* stand out as the most sensitive factors within the defined range of variations. It must be noted that *road density* is among the most sensitive factors for both standardization methods, although it is not the most sensitive in either of them.

K-S test results

As an alternative means to measure sensitivity, the K-S test was applied to the same simulations undertaken for the univariate SA, including range and interval variations. Regarding the K-S test applied to the weights-encoding method, the *p*-value (at an alpha value of 0.05) showed that 13 resulting landslide susceptibility map

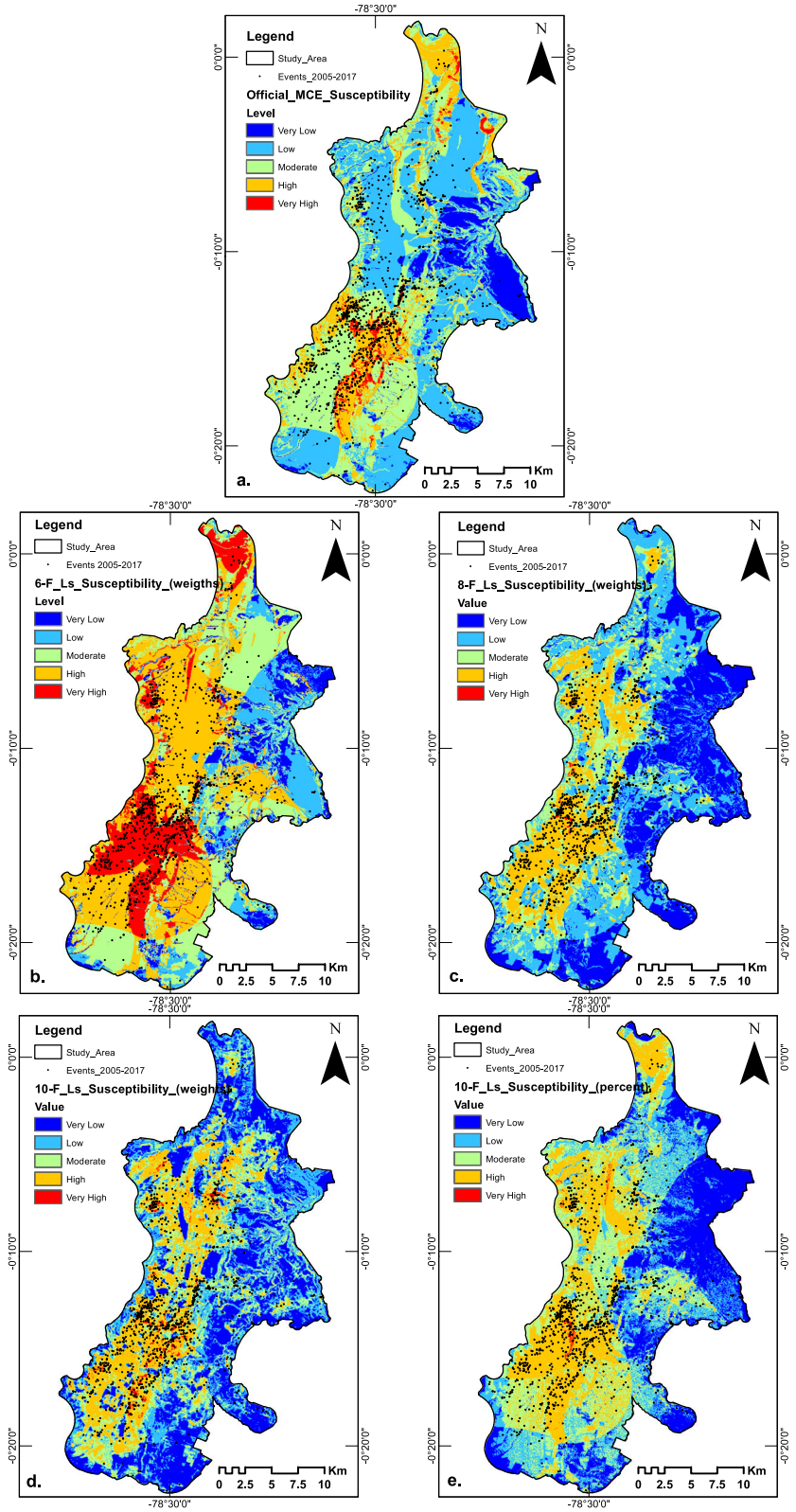


Fig. 3 (See legend on next page.)

(See figure on previous page.)

Fig. 3 Landslide susceptibility maps for Quito: **(a)** Multi-criteria evaluation (MCE) official map. From LOGIT modelling results: **(b)** Six-factor with weights encoding **(c)** Eight-factor with weights encoding **(d)** Ten-factor with weights encoding **(e)** Ten-factor with percentile discretization. Legend: All maps have been classified in 5 categories by the geometrical interval method in GIS (ArcMap 10.3). Other features: Study Area (black line), Landslide Events during the 2005–2017 period (black dots), and five classes of susceptibility levels (blue-yellow-red color spectrum)

samples, out of the 2000 simulated, were not significant. These 13 cases corresponded to variations in the coefficients of three factors: *road density*, *intense precipitations*, and *population* (see Fig. 6). For the percentile-discretized case, with the same alpha value, number of simulations, and range of variation, the resulting *p*-values showed that the results of their samples were non-significant only for two maps, with both samples corresponding to the *intense precipitations* factor coefficient variations. These results are illustrated in Fig. 7.

As mentioned in the methodology, the presentation of the values and charts of the D-statistic of the K-S test, also called the KS statistic, is more insightful as a measure of sensitivity. To illustrate these values and its correspondence with the *p*-values described above, the D-critical value ($D\alpha$) was calculated, which for both discretization methods was 0.057. The 13 non-significant samples, according to their *p*-values from the weights-discretization method cases, and the two non-significant samples, according to the *p*-values from the percentile-discretization method cases, can be identified in Fig. 8, corresponding to variations in the coefficients of the factors: *road density*, *intense precipitations*, and *population*. The high sensitivity of these factors is notable within the studied range of variation. The same can be appreciated in Fig. 9 for the percentile-discretized method cases. In this figure, two simulations, which are the non-significant samples, both corresponding to the *intense precipitations* factor coefficient variation, present D-statistic values below the critical $D\alpha = 0.057$. Similarly, in addition to this factor, *road density* and *building footprint* can also be appreciated as highly sensitive in Fig. 9.

Monte Carlo SA results

The second SA method was the random/stochastic method, also called Monte Carlo. The AUC value was, as previously discussed, used as a metric to test the

Table 7 Descriptive statistics of AUC values of LSM with LR for Quito for 100 simulations for cell sizes of 50, 100, 200, and 500 m

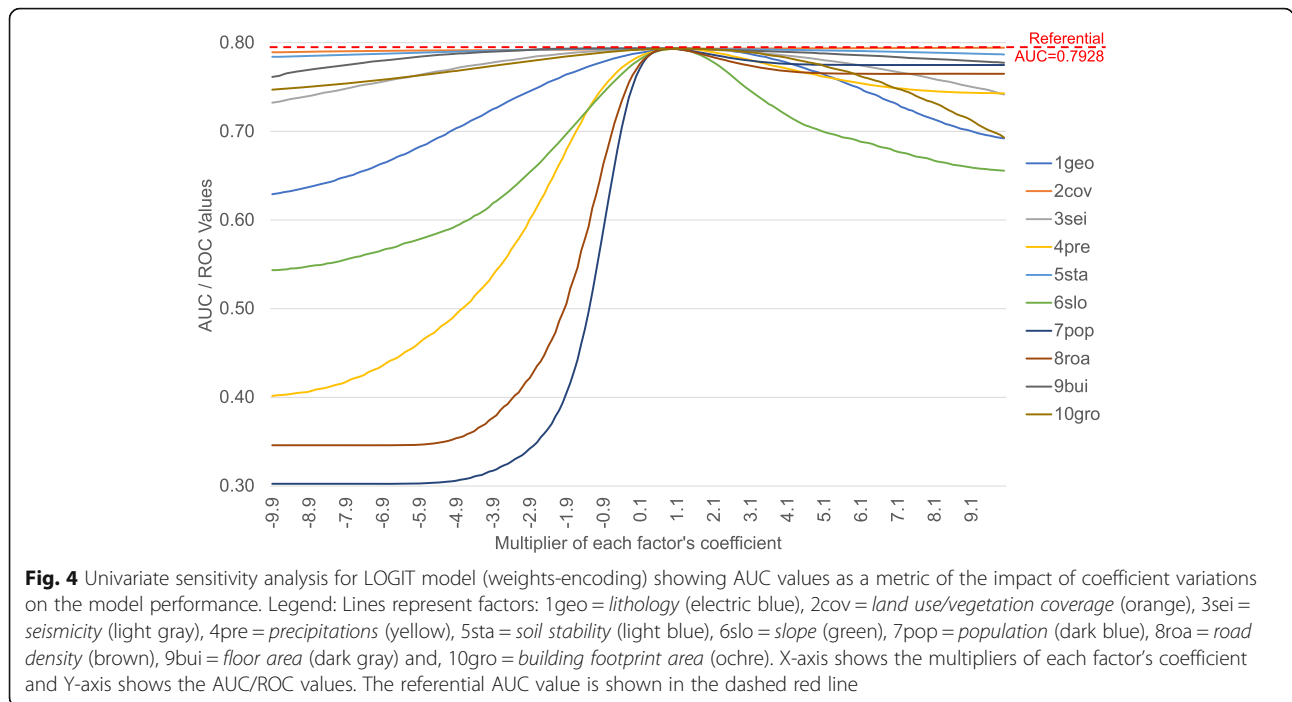
Cell size (m)	50	100	200	500
Average AUC value	0.7909	0.7833	0.8012	0.8277
Maximum AUC value	0.7965	0.7892	0.8133	0.9155
Minimum AUC value	0.7740	0.7699	0.7795	0.6034
Standard deviation	0.0052	0.0057	0.0062	0.0578
Range in 100 simulations	0.0226	0.0194	0.0338	0.3121

sensitivity for both weights and percentiles standardization methods. For each, 8000 simulations were produced. A difference can be seen between the weights and the percentile standardization methods' results. The weights-encoding model generated 350 AUC values (out of the 8000) that were higher than the reference of 0.7928, with the highest AUC = 0.7970, an improvement of 0.53% compared to the reference; whereas the percentile-discretized model generated 4440 values (out of the 8000) that were higher than the referential 0.7417, with a maximum AUC = 0.7968, an improvement of 7.43% compared to the reference. For the percentile-discretization case, a set of the highest 17, out of the 4440 possible combinations to change the reference coefficients, are presented in Table 8.

To provide a graphic example, the two factors with the highest values of coefficients (see Table 6) were selected to compare their AUC values with combinations from the variations of both coefficients, while the other eight coefficients maintained the reference values (*ceteris paribus*). They are illustrated in bubble charts to support the identification of the coordinates (combination) that performs with the highest AUC value. For the weights-encoding model these factors were *population* and *road density*, and the random outputs selected 12 combinations; however, none of these were higher than the reference (see Fig. 10). For the percentile-discretization model, the factors were *lithology* and *precipitations*, and the random outputs presented 18 combinations. In this last case, all combinations achieved higher AUC values than the reference (0.7417), as shown in Fig. 11

Discussion

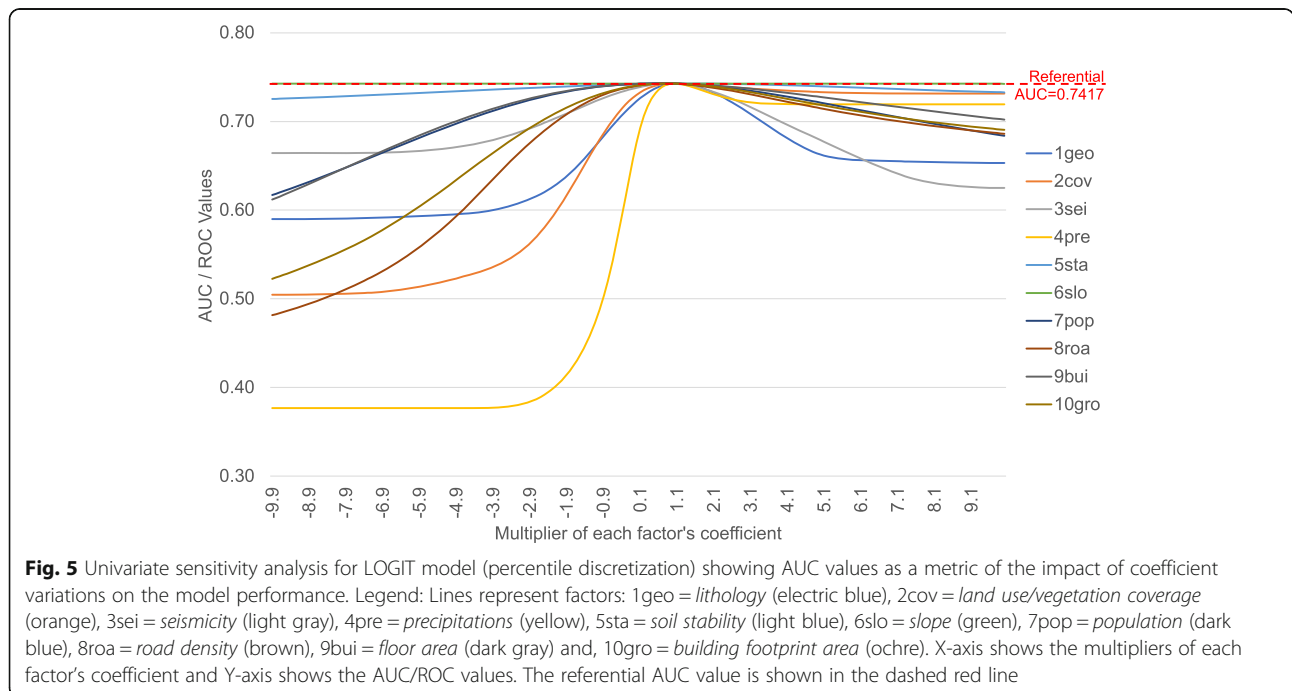
Prior to discussion of the particular component results and outcomes of this study, consideration should be given to the broad set of possible combinations of methodologies that a global LSM process, such as that presented, may adopt. Regardless of the modelling technique, it is relevant to consider the manner in which the data is generated and preprocessed as a parameter. In this regard, van Dessel et al. (2011) stress the impact of the quality of the input datasets on the resulting coefficients of logistic regression models applied to landslide susceptibility analysis. In this regard, when reviewing the quality of the data corresponding to *soil stability* and *seismic intensities*, it is notable that the level of detail is poor. This might limit the accuracy and performance of the models used in this study. Currently, micro-zoning seismicity studies are being



surveyed as part of a long-term project. In the future, this could help obtain precise results in LSM studies, in addition to better quality and newer data, which appears to be a promising development for Quito.

This research implemented a pseudo-quantitative method, which considered weights-encoded categorical data and discretized continuous data as inputs, previously assigned by official local experts. Data encoding is driven by

needs and expertise (Saltelli et al. 2019) of local DRM professionals and scholars. In this experiment, local knowledge was useful in gathering reliable data, regardless of potential distortions in the results, which can be enhanced and complemented by the statistical analysis of the empirical data itself (Grzenda 2020). In this regard, other studies have encoded data based on the frequency ratio of events of a specific class (Bui et al. 2020). For Quito, problems of



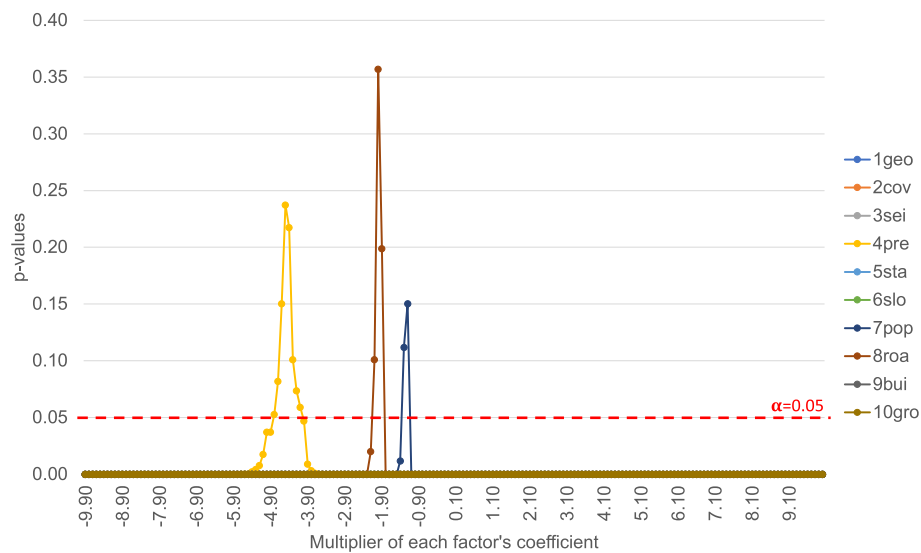


Fig. 6 This shows the *p*-values of the K-S test (two-sample) applied to 2000 landslide susceptibility datasets resulting from the univariate susceptibility analysis of the LOGIT model by weights discretization. Legend: The alpha value to determine the significance level was 0.05, which is marked with the dashed red line. The values (dots) above this level (*precipitations, population, and road density*) represent the non-significant samples from 13 simulations, whereas the remaining 1987 are considered to be at significance levels. The *building footprint* factor dots (ochre color) cover most of the dots representing these remaining simulations, which are very close to a *p*-value of zero. Lines with dots represent factors: 1geo = *lithology* (electric blue), 2cov = *land use/vegetation coverage* (orange), 3sei = *seismicity* (light gray), 4pre = *precipitations* (yellow), 5sta = *soil stability* (light blue), 6slo = *slope* (green), 7pop = *population* (dark blue), 8roa = *road density* (brown), 9bui = *floor area* (dark gray) and, 10gro = *building footprint area* (ochre). X-axis shows the multipliers of each factor's coefficient and Y-axis shows the *p*-values

unbalanced, unstructured, and underreported landslide events data are expected to be overcome in the future, thus improving weights encoding. Nevertheless, the encoded data was processed using a theoretical multicriteria assessment for LSM, as undertaken in other research works (Leoni et al. 2009; Lombardo and Mai 2018), which this study tested with a LOGIT model and SA, as described above.

For the current research, complementary data preparation was performed by scaling the factors' values based on both weight and percentile methods. In this regard, there are differences that should not be overlooked when running the LOGIT. For the first method (weights), the discretization scaling to the additional four "urban" factors enhanced the ROC/AUC value progressively, from 0.7550 to 0.7840, by adding population and floor area; and then to 0.7928 by adding road density and building footprint area. Nonetheless, when discretizing all ten factors to a percentile scale, the ROC/AUC value dropped to 0.7417, which is still acceptable in terms of the classification power of the model, but is not as reliable as the higher former value. Therefore, the discretization from a 1-to-4 weights scale to percentiles of the nominal factors did not provide accuracy. This may be because, for the 1-to-4 discrete weights scale, the only possible percentile values assigned were 1, 33, 67, and 100 (see Table 4), which affected the performance results of the model. In contrast, a broader scale, such as that of the percentiles, normally provides better parameterization

possibilities and, therefore, global performance, than the cost-sensitive LOGIT model (Zhang et al. 2020).

In addition to using data provided by the municipality of Quito, this research included more factors than the official landslide susceptibility study. These factors were *population, road density, floor area, and building footprint area*, which we consider helped to characterize the urban category from the *land use/vegetation coverage* factor of the former study. This can be seen by observing the progressive change in the order of coefficients and AUC values in Table 6.

In relation to the urban variables, it can be expected that *population*, which appeared as an important predictor after the LOGIT application, may be related to *building footprint area* and *floor area*. Nonetheless, the latter factors were not found to be relevant predictors. This might be related to the fact that the largest floor area volumes are concentrated on the center-north of the city, an area where self-built and informal construction is low, and buildings are often medium-rise with appropriate construction techniques, soil management, and artificial drainage. A further step of this study could include factors to assess LSM at building scales, using a vulnerability and uncertainty quantification approach, and considering the heterogeneity of urban fabrics, such as those undertaken by Kaynia et al. (2008) and Du et al. (2013). This research additionally may enhance the data quality in surveying building conditions and soil

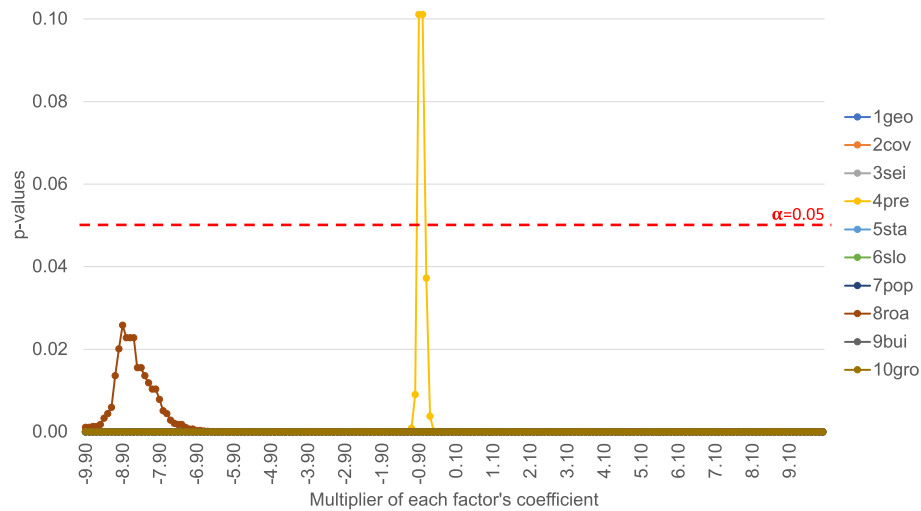


Fig. 7 This shows the *p*-values of the K-S test (two-sample) applied to 2000 landslide susceptibility datasets resulting from the univariate susceptibility analysis of the LOGIT model by percentile discretization. Legend: The alpha value to determine the significance level was 0.05, which is marked with the dashed red line. The values (dots) above this level (*precipitations*) represent the non-significant samples from two simulations, whereas the remaining 1998 are considered to be at significance levels. The *building footprint* factor dots (ochre color) cover most of the dots representing these remaining simulations, which are very close to a *p*-value of zero. Lines with dots represent factors: 1geo = *lithology* (electric blue), 2cov = *land use/vegetation coverage* (orange), 3sei = *seismicity* (light gray), 4pre = *precipitations* (yellow), 5sta = *soil stability* (light blue), 6slo = *slope* (green), 7pop = *population* (dark blue), 8roa = *road density* (brown), 9bui = *floor area* (dark gray) and, 10gro = *building footprint area* (ochre). X-axis shows the multipliers of each factor's coefficient and Y-axis shows the *p*-values

management, and data collection at a large urban scale, as for the case of Quito.

Another complementary remark regarding the results in terms of policy implications is that the relevance of the *road density* factor as a predictor does

not necessarily mean that streets and roads per se increase LRisk. In fact, heterogeneity can have an important effect on the model (Wang et al. 2020). Because roads are potential boosters of urban development, it is necessary to examine in detail how

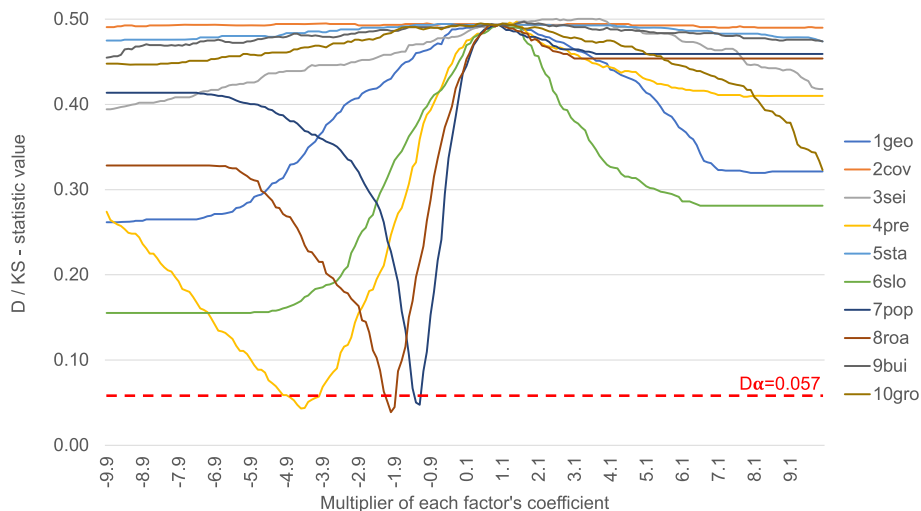


Fig. 8 This shows the D-statistic values of the two-sample K-S test for univariate sensitivity analysis of 2000 simulations, by weights discretization. Legend: The critical value (D_{α}), related to an alpha value of 0.05, is marked with the dashed red line. The values below this level (*precipitations*, *population*, and *road density*) represent the non-significant samples from 13 simulations, whereas the remaining 1987, represented above the line, are considered to be at significance levels. Lines represent factors: 1geo = *lithology* (electric blue), 2cov = *land use/vegetation coverage* (orange), 3sei = *seismicity* (light gray), 4pre = *precipitations* (yellow), 5sta = *soil stability* (light blue), 6slo = *slope* (green), 7pop = *population* (dark blue), 8roa = *road density* (brown), 9bui = *floor area* (dark gray) and, 10gro = *building footprint area* (ochre). X-axis shows the multipliers of each factor's coefficient and Y-axis shows the D/KS values

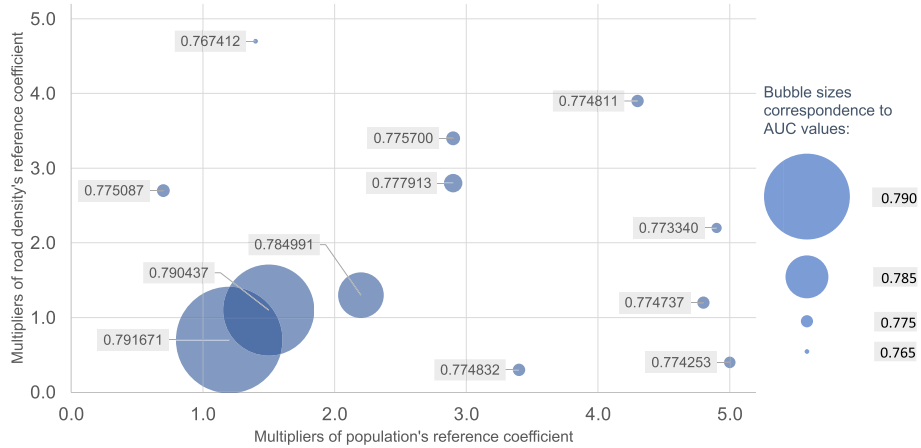


Fig. 10 AUC values resulting from random combinations of *population* and *road density* coefficients' variations of the reference outputs of the weights-encoding LOGIT model. Legend: Blue bubble sizes represent the AUC values, whose area has been magnified according to the artifice $(AUC \cdot 10)^{200}$. X-axis shows the multipliers of the *population* factor's reference coefficients and Y-axis shows the multipliers of the *road density* factor's reference coefficients

vulnerability is produced at the household scale, as mentioned above.

Conclusions

This article presented the application of a binary logistic regression model with the objective of producing a landslide susceptibility map for the urban area of Quito, Ecuador. A landslide events database covering the 2005–2017 period was used as the dependent binary factor. Ten explanatory factors were tested: *lithology*, *land use / vegetation coverage*, *seismic intensities*, *intense precipitations*, *soil stability based on previous events*, *slope*, *population*, *road density*, *floor area*, and *building footprint area*. Adding the last four factors—considered “urban”—

was found to result in better performance of the model (AUC = 0.7928) compared to the model operating only with the first six factors (AUC = 0.7550).

Two data standardization methods were applied: weights encoding and percentile discretization. After operating the LOGIT model, the weighted-encoding method delivered an AUC of 0.7928, whereas the percentile-discretized model obtained 0.7417. Regarding the resulting coefficients of the explanatory factors, the weights-encoding method provided more stable values than the percentile-discretized approach, whose performance delivered greater oscillation in the coefficient values, after several simulations. The instability in the second method may be due to large differences in the

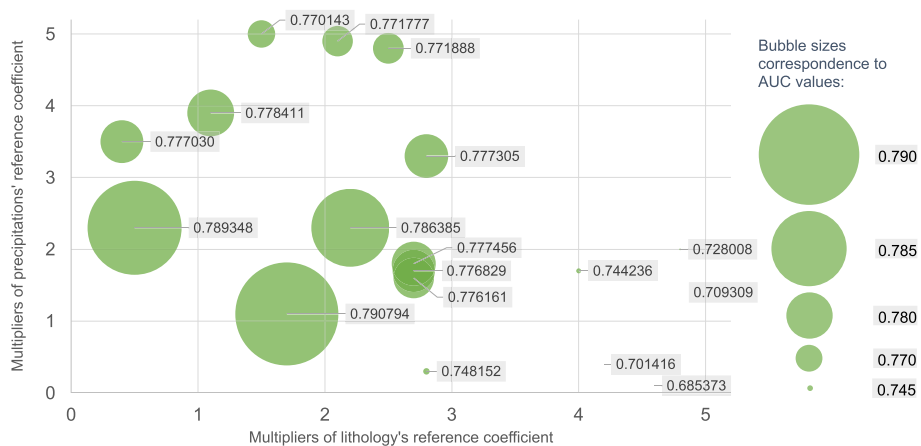


Fig. 11 AUC values resulting from random combinations of *lithology* and *precipitations* coefficients' variations of the reference outputs from the percentile-discretization LOGIT model. Legend: Green bubble sizes represent the AUC values, whose area has been magnified according to the artifice $(AUC \cdot 100)^{100}$. X-axis show the multipliers of the *lithology* factor's reference coefficients and Y-axis show the multipliers of the *precipitations* factor's reference coefficients

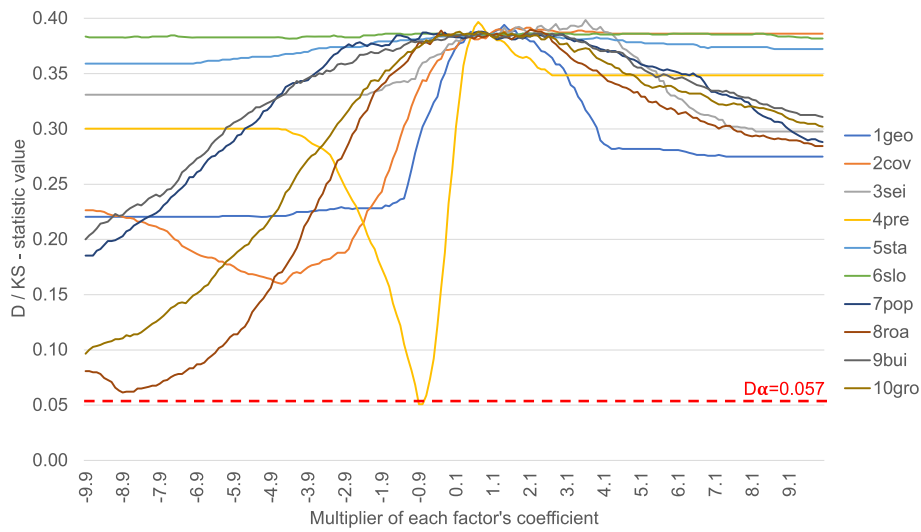


Fig. 9 This shows the D-statistic values of the two-sample K-S test for univariate sensitivity analysis of 2000 simulations, by percentile discretization. Legend: The critical value (D_{α}), related to an alpha value of 0.05, is marked with the dashed red line. The values below this level (precipitations) represent the non-significant samples from two simulations, whereas the remaining 1998, represented above the line, are considered to be at significance levels. Lines represent factors: 1geo = lithology (electric blue), 2cov = land use/vegetation coverage (orange), 3sei = seismicity (light gray), 4pre = precipitations (yellow), 5sta = soil stability (light blue), 6slo = slope (green), 7pop = population (dark blue), 8roa = road density (brown), 9bui = floor area (dark gray) and, 10gro = building footprint area (ochre). X-axis shows the multipliers of each factor's coefficient and Y-axis shows the D/KS values

Table 8 Randomly selected combination of multipliers of coefficients of the LOGIT model (percentile-discretized) to calibrate it for optimal results in defining the landslide susceptibility map

AUC	Lithology	Land Use/Veg Cover	Seismic Intensity	Intense Precipitations	Soil Stability	Slope	Population	Road Density	Floor Area	Building Footprint
0.74170 ^b	0.01600 ^a	0.01220 ^a	- 0.01100 ^a	0.02380 ^a	0.00470 ^a	- 0.00045 ^a	0.00340 ^a	0.00520 ^a	- 0.00400 ^a	- 0.00380 ^a
0.79682	1	1	1	1.3	1	1	1	1	1	1
0.79682	1	1	1	1.3	1	1	1	1	1	1
0.79676	1	1	1	1.4	1	1	1	1	1	1
0.79676	1	1	1	1.4	1	1	1	1	1	1
0.79676	1	1	1	1.4	1	1	1	1	1	1
0.79671	1	1.5	1.4	1.3	1	1	1	1	1.9	1
0.79667	1	1	1	1.2	1	1	1	1	1	1
0.79667	1	1	1	1.2	1	1	1	1	1	1
0.79662	1	1	1	1.4	3.9	1	1	1	1	1
0.79655	1	1	1	1.5	3.1	1	1	1	0.3	1
0.79653	1	1	1	1.1	1	1	1	1	1	1
0.79653	1	1	1	1.1	1	1	1	1	1	1
0.79651	3.4	4.2	1.6	3.9	0.1	4.1	3.1	3.7	2.9	1.1
0.79651	1	1	1	1.1	1.8	1	1	1	1	1
0.79651	1	1	1	1.1	1.8	1	1	1	1	1
0.79646	0.9	1	1	1	1	1	1	1	1	1
0.79646	0.9	1	1	1	1	1	1	1	1	1

^aThe reference coefficients for each factor provided from the initial LOGIT model application (percentile-discretization)

^bThe reference AUC values provided after the initial LOGIT model application (percentile-discretization)

percentiles' classification, particularly for the categorical data. According to the results of the weights-encoding method, which was the most stable model, the factors of *road density*, *population*, *intense precipitations*, and *slope*, in that order, improved the prediction/classification power. The percentiles-discretization method (least stable model) showed that *intense precipitations*, *lithology*, *land use/vegetation coverage*, and *road density*, in that order, provided the best prediction improvement.

Concerns about the resolution were addressed by testing changes of this parameter for cell sizes of 50 (the originally generated input), 100, 200, and 500 m. Results showed that, even when the highest values are achieved with smaller resolutions, this behavior is not stable when producing several simulations. In contrast, the 50 m cell size model remains stable, whereas its performance according to the AUC value (0.7928) demonstrates a high classification power. Hence, this resolution was chosen for the sensitivity analysis.

Univariate, Monte Carlo and K-S tests were applied to measure the sensitivity of factors (both standardization methods). AUC was used to measure the performance for the first two tests and the K-statistic for the final test. From the univariate SA results, it can be observed that the *slope*, *road density*, *intense precipitations*, and *population* factors curves resulted in the widest variations. This was the case for the weights-encoded method (see Fig. 4). In the case of the percentile-discretized method (see Fig. 5), the most sensitive factor curves were those of *intense precipitations*, *land use/vegetation coverage*, *lithology*, and *road density*, within the studied simulation range. Moreover, 241 out of 2000 simulations provided better calibration of the weights-encoded model, with a 0.2% improvement of the AUC value; and 34 out of 2000 simulations provided better calibration of the percentile-discretization model, but with only a marginal 0.03% improvement of the AUC value.

Regarding the Monte Carlo SA for the weights-encoding model, 350 out of 8000 simulations showed higher AUC values than the reference value, improving on it by up to 0.53%. This differs substantially from the weights-normalized model, which in the Monte Carlo application only resulted in 4440 AUC values that were higher than the reference, improving on it by up to 7.4%. This means that the calibration of the percentile-normalized model's coefficients can still be adjusted to improve predictability. Nonetheless, it does not achieve significant better performance than the weights-encoding model.

Finally, a two-sample K-S test was used to measure sensitivity, using the D-statistic as a metric, and using the same univariate SA simulations. In contrast to the univariate and Monte Carlo SAs, the K-S test indicated that, for the weights' method, 13 simulations in the weights-

encoded cases were not significant in classification power at $\alpha = 0.05$, with the variations of *road density*, *precipitations*, and *population* coefficients being sensitive beyond the D-critical value. For the percentile-discretization cases, only two simulations were not significant, with *precipitations* as the sensitive factor, using the same alpha value.

This research aimed to contribute to the study of LSM, not only with the inclusion of Quito as an Andean city in an LRisk context, but also by observing LR modelling behavior when incorporating novel "urban" factors, which is rarely found in the LSM literature. In this regard, results highlight the importance of the *street/road network* and *population* factors on the overall classification power of the model. In contrast, the building-related factors (i.e., *floor area* and *building footprint*) do not appear to have the same influence and their inverse effect remains to be explored. Other factors, such as *slope* and *rainfall*, appeared to be relatively relevant in the LOGIT-LSM in this urban context, although the quality of the local geology, for the most part, helps to reduce the incidence of LRisk, according to local experts.

It is expected that further research for the case of Quito and similar Andean cities will benefit from the generation of better quality and more detailed official data, particularly regarding factors addressing the urban form and physical and social vulnerability. Ultimately, improved performance of LSM may support LRR policy design, considering the diverse implications that accurate delimitation of risk zones has for LRisk generation, in addition to making land suitable for LRR, the construction of safe housing, and urban development.

Abbreviations

AHP: Analytical hierarchical process; ANN: Artificial neural networks; AUC: Area under the curve (ROC value); CF: Certainty factor; COE-M: Metropolitan Emergency Operations Committee of Quito; DL: Deep learning; DMQ: Metropolitan District of Quito; DRM: Disaster risk management; DRR: Disaster risk reduction; DTM: Digital terrain model; EMS: European Macroseismic Scale; EPMMOP: Empresa Pública Metropolitana de Movilidad y Obras Públicas (Metropolitan Public Enterprise of Mobility and Public Works of Quito); FFNN: Feed-forward neural network; FR: Data-driven frequency ratio; GIS: Geographic information systems; IGM: Instituto Geográfico Militar Ecuador (Military Geography Institute of Ecuador); INEC: Instituto Nacional de Estadísticas y Censos de Ecuador (National Institute of Statistics and Census of Ecuador); IV: Information value; JT: Jackknife test; K-S: Kolmogorov-Smirnov test; LCVs: Landslide conditioning factors; LOGIT: Binary logistic regression model; LR: Logistic regression; LRisk: Landslide risk; LRR: Landslide risk reduction; LS: Landslide susceptibility; LSI: Landslide susceptibility index; LSM: Landslide susceptibility mapping or landslide susceptibility map; LUP: Land-use planning; MCE: Multi-criteria evaluation; MDMQ: Municipio del Distrito Metropolitano de Quito (Government of the Metropolitan District of Quito); ML: Maximum likelihood; MuF: Multiple factor model; MURs: Mapping unit resolutions; NDVI: Normalized difference vegetation index; OAT: One-At-a-Time; OB: Object based approaches; OWA: Ordered weighted average; PBA: Pixel based approaches; PEI: Potential erosion index; PRE: Potential rain effect; RF: Random forest; ROC: Receiving operator characteristic; SA: Sensitivity analysis; SGP: Secretaría General de Planificación (Secretariat of General Planning of the MDMQ); SI: Susceptibility index; SPI: Stream power index; SSG: Secretaría de Seguridad y Gobernabilidad (Secretariat of Security and

Governability of the MDMQ); STHV: Secretaría de Territorio, Hábitat y Vivienda (Secretariat of Territory, Habitat and Housing of the MDMQ); SVM: Support vector machine; TPI: Topographic position index; TRI: Topographic roughness index; TWI: Topographic wetness index; WeF: Weight factor model; WLC: Weighted linear combination; ZR: Landslide Risk Zone or "Zona de Riesgo" (a LUP category in Quito)

Supplementary Information

The online version contains supplementary material available at <https://doi.org/10.1186/s40677-021-00184-0>.

Additional file 1. 08_codes_link.

Additional file 2. 10_figsedit_link.

Acknowledgements

The authors would like to acknowledge the support from the Secretariat of Security and Governability of the Municipality of Quito (MDMQ-SSG) and the National Institute of Statistics and Census of Ecuador (INEC) in providing the data. This research is possible thanks to a PhD scholarship granted under the Agreement of Institutional Support between the Universidad Central del Ecuador (UCE) and the Académie De Recherche Et D'Enseignement Supérieur (ARES) from Belgium. The authors would also like to acknowledge the support of Frédéric Collin and Mario Cools (Liège University), Jorge Ordóñez (MDMQ-SSG), and Marco Rivera and Galo Plaza (independent consultants), who provided scientific/technical advice for the analysis. Finally, the contribution of anonymous reviewers was fundamental for the improvement of the former version of this work.

Code availability

Code was developed by Fernando Puente-Sotomayor, with the advice of Ahmed Mustafa and Jacques Teller. It is provided as supplementary material. Further requests can be submitted to the corresponding author.

Authors' contributions

Fernando Puente-Sotomayor: Conceptualization; Data curation; Formal analysis; Funding acquisition; Investigation; Methodology; Project administration; Resources; Visualization; Writing - original draft. Ahmed Mustafa: Methodology; Software; Supervision; Validation; Writing - review & editing. Jacques Teller: Conceptualization; Formal analysis; Funding acquisition; Investigation; Methodology; Project administration; Resources; Supervision; Validation; Writing - review & editing. The authors read and approved the final manuscript.

Funding

This research was funded as part of a PhD study supported by the Agreement of Institutional Support between the Universidad Central Ecuador and the Académie De Recherche Et D'Enseignement Supérieur from Belgium, of which Liège University is the member hosting the study.

Availability of data and materials

Data used and processed for this study comes all from secondary sources. These sources are the Metropolitan District of Quito, from which part of the data is open to the public through the official website, and variables containing data about *slope*, *stability*, *lithology*, *land coverage*, *precipitations* and *seismicity* were officially requested and delivered by the institution. Datasets of the *population* and road density factors were downloaded through the official website of the National Statistics and Census Bureau of Ecuador (INEC).

Declarations

Competing interests

The authors declare they have no conflicts of interest or competing interests in the present study.

Author details

¹Local Environmental Management and Analysis (LEMA), Urban and Environmental Engineering Dept., Liège University, Liège, Belgium. ²Facultad de Arquitectura y Urbanismo, Universidad Central del Ecuador, Quito,

Ecuador. ³Urban Systems Lab, The New School University, New York, NY, USA.

Received: 14 August 2020 Accepted: 20 April 2021

Published online: 20 August 2021

References

- Bathrellos GD, Kalivas DP, Skilodimou HD (2009) GIS-based landslide susceptibility mapping models applied to natural and urban planning in Trikala, Central Greece. *Estud Geol* 65(1):49–65. <https://doi.org/10.3989/egcol.08642.036>
- Blanchard-Boehm RD (2004) Natural hazards in Latin America: tectonic forces and storm fury. *Soc Stud* 95(3):93–105. <https://doi.org/10.3200/TSS5.95.3.93-105>
- Bouyer J (2009) Modélisation et simulation des microclimats urbains: Étude de l'impact de l'aménagement urbain sur les consommations énergétiques des bâtiments. Thèse, Université de Nantes. <https://tel.archives-ouvertes.fr/tel-00426508>. Accessed 25 Dec 2019
- Bui DT, Tsangaratos P, Nguyen VT, Van Liem N, Trinh PT (2020) Comparing the prediction performance of a deep learning neural network model with conventional machine learning models in landslide susceptibility assessment. *Catena* 188:104426. <https://doi.org/10.1016/j.catena.2019.104426>
- Catani F, Lagomarsino D, Segoni S, Tofani V (2013a) Exploring model sensitivity issues across different scales in landslide susceptibility. *Nat Hazards Earth Syst Sci Discuss* 1(2):583–623. <https://nhess.copernicus.org/preprints/1/583/2013/nhessd-1-583-2013.pdf>
- Catani F, Lagomarsino D, Segoni S, Tofani V (2013b) Landslide susceptibility estimation by random forests technique: sensitivity and scaling issues. *Nat Hazards Earth Syst Sci* 13(11):2815–2831. <https://doi.org/10.5194/nhess-13-2815-2013>
- Chang KT, Merghadi A, Yunus AP, Pham BT, Dou J (2019) Evaluating scale effects of topographic variables in landslide susceptibility models using GIS-based machine learning techniques. *Sci Rep* 9(1):1–21. <https://doi.org/10.1038/s41598-019-48773-2>
- Comunidad Andina (2017) Estrategia Andina para la Gestión del Riesgo de Desastres - Decisión No. 819. <http://www.comunidadandina.org/StaticFiles/2017522151956ESTRATEGIAANDINA.pdf>. Accessed 20 Feb 2020
- D'Ercole R, Hardy S, Metzger P, Robert J (2009) Vulnerabilidades urbanas en los países andinos. Introducción general. *Bull l'Institut Français d'études Andines* 38(3):401–410. <https://doi.org/10.4000/bifea.2222>
- Dragičević S, Lai T, Balram S (2015) GIS-based multicriteria evaluation with multiscale analysis to characterize urban landslide susceptibility in data-scarce environments. *Habitat Int* 45(P2):114–125. <https://doi.org/10.1016/j.habitatint.2014.06.031>
- Du G, Zhang Y, Iqbal J, Yang Z, Yao X (2017) Landslide susceptibility mapping using an integrated model of information value method and logistic regression in the Bailongjiang watershed, Gansu Province, China. *J Mt Sci* 14(2):249–268. <https://doi.org/10.1007/s11629-016-4126-9>
- Du J, Yin K, Nadim F, Lacasse S (2013) Quantitative vulnerability estimation for individual landslides. In P. des Ponts (Ed.), Proceedings of the 18th international conference on soil mechanics and geotechnical engineering, Paris 2013 (pp. 2181–2184). <http://www.cfms-sols.org/sites/default/files/Actes/2181-2184.pdf>. Accessed 4 Jan 2020
- Ecuador Asamblea Nacional (2014) Ley Orgánica Reformativa al Código Orgánico de Organización Territorial, Autonomía y Descentralización. <http://www.misionpichincha.gob.ec/transparencia/organizacion-interna-base-legal/normasderegulacion/pdfs/RegistroOficial166LeyReformatoriaalCootad.pdf>. Accessed 2 Apr 2020
- Feizizadeh B, Blaschke T (2014) An uncertainty and sensitivity analysis approach for GIS-based multicriteria landslide susceptibility mapping. *Int J Geogr Inf Sci* 28(3):610–638. <https://doi.org/10.1080/13658816.2013.869821>
- FUNEPSA, Rivera M, Salazar A, Carvajal A, Galárraga R, Plaza G, Singaucha JC, Álvarez B, Salazar D (2015) Actualización de la Zonificación por Amenaza de Deslizamiento en el Distrito Metropolitano de Quito. SSG-MDMQ Official Report, Quito
- GEMMA (2007) Movimientos en masa en la región Andina: Una guía para la evaluación de amenazas. Servicio Nacional de Geología y Minería 4:432. <http://bypad.indeci.gob.pe/doc/pdf/esp/doc2212/doc2212.htm>. Accessed 19 Dec 2019
- Grzenda, W (2020) The role of discretization of continuous variables in socioeconomic classification models on the example of logistic regression models and artificial neural networks. In K. Jajuga, J. Batóg, & M. Walesiak (Eds.), Classification and Data Analysis. Theory and Applications (first, pp. 35–52). Cham: Springer

- Gudiyangada Nachappa T, Kienberger S, Meena SR, Hölbling D, Blaschke T (2020) Comparison and validation of per-pixel and object-based approaches for landslide susceptibility mapping. *Geomatics Nat Hazards Risk* 11(1):572–600. <https://doi.org/10.1080/19475705.2020.1736190>
- Hemasinghe H, Rangali RSS, Deshapriya NL, Samarakoon L (2018) Landslide susceptibility mapping using logistic regression model (a case study in Badulla District, Sri Lanka). *Proc Eng* 212:1046–1053. <https://doi.org/10.1016/j.proeng.2018.01.135>
- Highland LM, Bobrowsky P (2008) *The Landslide Handbook — A Guide to Understanding Landslides*. US Geological Survey Circular 1325, Reston. https://pubs.usgs.gov/circ/1325/pdf/C1325_508.pdf. Accessed 12 Nov 2019
- INEC (2016) Proyección Cantonal Total 2010–2020. INEC Registry. http://www.inec.gob.ec/estadisticas/index.php?option=com_content&view=article&id=329&Itemid=328&lang=es. Accessed 12 Nov 2019
- Inostroza L (2017) Informal urban development in Latin American urban peripheries. Spatial assessment in Bogota, Lima and Santiago de Chile. *Landscape Urban Plan* 165(1):267–279. <https://doi.org/10.1016/j.landurbplan.2016.03.021>
- Kaynia AM, Paphthoma-Köhle M, Neuhaus B, Ratzinger K, Wenzel H, Medina-Cetina Z (2008) Probabilistic assessment of vulnerability to landslide: application to the village of Lichtenstein, Baden-Württemberg, Germany. *Eng Geol* 101(1–2):33–48. <https://doi.org/10.1016/j.enggeo.2008.03.008>
- Kirschbaum D, Stanley T (2018) Satellite-based assessment of rainfall-triggered landslide Hazard for situational awareness. *Earth's Future* 6(3):505–23. <https://doi.org/10.1002/2017EF00071>
- Klimeš J, Rios Escobar V (2010) A landslide susceptibility assessment in urban areas based on existing data: an example from the Iguaná Valley, Medellín City, Colombia. *Natural Hazards Earth Syst Sci* 10(10):2067–2079. <https://doi.org/10.5194/nhess-10-2067-2010>
- Lara M, Sepúlveda SA, Celis C, Rebolledo S, Ceballos P (2018) Landslide susceptibility maps of Santiago city, Andean foothills, Chile. *Andean Geol* 45(3):433–442. <https://doi.org/10.5027/andgeoV45n3-3151>
- Lee S, Baek WK, Jung HS, Lee S (2020) Susceptibility mapping on urban landslides using deep learning approaches in mt. Umyeon. *Appl Sci* 10(22):1–18. <https://doi.org/10.3390/app10228189>
- Leoni G, Barchiesi F, Catalo F, Dramis F, Fubelli G, Lucifora S, Mattei M, Pezzo G, Puglisi C (2009) GIS methodology to assess landslide susceptibility: application to a river catchment of Central Italy. *J Maps* 5(1):87–93. <https://doi.org/10.4113/jom.2009.1041>
- Lombardo L, Mai PM (2018) Presenting logistic regression-based landslide susceptibility results. *Eng Geol* 244(January):14–24. <https://doi.org/10.1016/j.enggeo.2018.07.019>
- Meena SR, Ghorbanzadeh O, Blaschke T (2019) A comparative study of statistics-based landslide susceptibility models: a case study of the region affected by the Gorkha earthquake in Nepal. *ISPRS Int J Geo Inf* 8(2). <https://doi.org/10.3390/ijgi8020094>
- Melchiorre C, Castellanos Abella EA, van Westen CJ, Matteucci M (2011) Evaluation of prediction capability, robustness, and sensitivity in non-linear landslide susceptibility models, Guantánamo, Cuba. *Comput Geosci* 37(4):410–425. <https://doi.org/10.1016/j.cageo.2010.10.004>
- Norman G (2010) Likert scales, levels of measurement and the “laws” of statistics. *Adv Health Sci Educ* 15(5):625–632. <https://doi.org/10.1007/s10459-010-9222-y>
- Orán Cáceres JP, Gómez Delgado M, Bosque Sendra J (2010) Una propuesta complementaria de análisis de sensibilidad de un modelo basado en técnicas sig y evaluación multicriterio. *Pubs. Univ. de Sevilla*. 2010(14):971–987. <http://hdl.handle.net/11441/66681>. Accessed 21 Nov 2019
- Pascale S, Parisi S, Mancini A, Schiattarella M, Conforti M, Sole A, Murgante B, Sdao F (2013) Landslide susceptibility mapping using artificial neural network in the urban area of Senise and San Costantino Albanese (Basilicata, southern Italy). In: Murgante B. et al. (eds) *Computational Science and Its Applications*. ICCSA 2013. Lecture Notes in Computer Science. Springer, Berlin, Heidelberg (pp. 473–488). https://doi.org/10.1007/978-3-642-39649-6_34
- Pasta DJ (2009) Learning when to be discrete: continuous vs. categorical predictors. In: *SAS Global Forum 2009, Statistics and Data Analysis*. 2009 Mar (p. 248). <https://support.sas.com/resources/papers/proceedings09/248-2009.pdf>. Accessed 19 Nov 2019
- Pawluszek K, Borkowski A, Tarolli P (2018) Sensitivity analysis of automatic landslide mapping: numerical experiments towards the best solution. *Landslides* 15(9):1851–1865. <https://doi.org/10.1007/s10346-018-0986-0>
- Poelmans L, Van Rompaey A (2010) Complexity and performance of urban expansion models. *Comput Environ Urban Syst* 34(1):17–27. <https://doi.org/10.1016/j.compenurbysys.2009.06.001>
- Puente-Sotomayor F, Egas A, Teller J (2021) Land policies for landslide risk reduction in Andean cities. *Habitat International* 107(Jan):102298. <https://doi.org/10.1016/j.habitatint.2020.102298>
- Puente-Sotomayor F, Villamarin P, Cevallos A (2018) Riesgos de deslizamiento en Quito, ¿funciona la política? In: *Asociación Geográfica del Ecuador (ed) Territorios en transición: Transformaciones de la Geografía del Ecuador en el siglo XXI - Memorias del 1er Congreso Nacional de Geografía del Ecuador*. Asociación Geográfica del Ecuador, Quito, pp 1–15. https://congresonacionlagec.files.wordpress.com/2018/02/memoria_cng_2018.pdf. Accessed 15 Dec 2019.
- Psomiadis E, Papazachariou A, Soulis KX, Alexiou DS, Charalampopoulos I (2020) Landslide mapping and susceptibility assessment using geospatial analysis and earth observation data. *Land* 9(5):133. <https://doi.org/10.3390/land9050133>
- Quito Alcaldía del Distrito Metropolitano (2018) Resolución Administrativa A008, Ordenanzas y Resoluciones 1–5 (2018). http://www7.quito.gob.ec/mdmq_ordenanzas/Resoluciones de Alcaldía/Año 2018/RA-2018-008-DIRECCION METROPOLITANA DE RESILIENCIA/CREACION.PDF. Accessed 20 Feb 2020
- Quito Concejo del Distrito Metropolitano (2003) Ordenanza Metropolitana No. 095 Régimen de Suelo. http://www7.quito.gob.ec/mdmq_ordenanzas/Ordenanzas/ORDENANZAS AÑOS ANTERIORES/ORDM-095 - NUEVO REGIMEN DELSUELO.pdf. Accessed 15 Dec 2019
- Quito Concejo del Distrito Metropolitano (2011) Ordenanza Metropolitana No. 172 Régimen de Suelo de Quito. [http://www7.quito.gob.ec/mdmq_ordenanzas/ConcejoAbierto/Ordenanzas/ORDENANZAS/MUNICIPALES/MUNICIPAL\(172\)/MUNICIPAL_0172_517.pdf](http://www7.quito.gob.ec/mdmq_ordenanzas/ConcejoAbierto/Ordenanzas/ORDENANZAS/MUNICIPALES/MUNICIPAL(172)/MUNICIPAL_0172_517.pdf). Accessed 4 Jan 2020.
- Quito Municipio del Distrito Metropolitano (2015) Plan de Desarrollo y Ordenamiento Territorial 2015 - Diagnóstico Eje Territorial. MDMQ. http://www7.quito.gob.ec/mdmq_ordenanzas/Sesiones del Concejo/2015/Sesión Extraordinaria 2015-02-13/PMDOT 2015-2025/Volumen I/6. Diagnóstico Territorial.pdf. Accessed 12 Nov 2019
- Quito Municipio del Distrito Metropolitano (2017) Estrategia de Resiliencia Distrito Metropolitano de Quito. MDMQ. <http://www.pichincha.gob.ec/pichincha/cantones/item/23-distrito-metropolitano-de-quito.html>. Accessed 21 Nov 2019
- Ramos-Bernal RN, Vázquez-Jiménez R, Sánchez Tizapa S, Arroyo Matus R (2019) Characterization of susceptible landslide zones by an accumulated index. In: R. Ram & M. Lazzari (Eds.), *Landslides - Investigation and Monitoring* (first, pp. 1–26). Intech Open. <https://www.intechopen.com/books/advanced-biometric-technologies/liveness-detection-in-biometrics>. Accessed 12 Feb 2020
- Rebotier J (2016) El Riesgo y su Gestión en Ecuador - Una Mirada de Geografía Social y Política. Centro de Publicaciones Pontificia Universidad Católica del Ecuador, Quito. https://biblio.flacsoandes.edu.ec/shared/biblio_view.php?bibid=143165&tab=opac. Accessed 15 May 2018.
- Reichenbach P, Rossi M, Malamud BD, Mihir M, Guzzetti F (2018) A review of statistically-based landslide susceptibility models. *Earth Sci Rev* 180(March):60–91. <https://doi.org/10.1016/j.earscirev.2018.03.001>
- Ronchetti F, Corsini A, Kollarits S, Leber D, Papez J, Plunger K, Preseren T, Schnetzer I, Stefani M (2013) Improve information provision for disaster management: MONITOR II, EU project. In: Margottini C, Canuti P, Sassa K (eds) *Landslide science and practice, Social and Economic Impact and Policies*, vol 7. Springer, Rome, pp 47–54. https://doi.org/10.1007/978-3-642-31313-4_7
- Saltelli A, Aleksankina K, Becker W, Fennell P, Ferretti F, Holst N, Li S, Wu Q (2019) Why so many published sensitivity analyses are false: a systematic review of sensitivity analysis practices. *Environ Model Softw*, 114(2019):29–39. <https://doi.org/10.1016/j.envsoft.2019.01.012>
- Shahabi H, Hashim M (2015) Landslide susceptibility mapping using GIS-based statistical models and remote sensing data in tropical environment. *Sci Rep* 5:1–15. <https://doi.org/10.1038/srep09899>
- Shahri AA, Spross J, Johansson F, Larsson S (2019) Landslide susceptibility hazard map in Southwest Sweden using artificial neural network. *Catena* 183(2019):104225. <https://doi.org/10.1016/j.catena.2019.104225>
- Sepúlveda SA, Petley DN (2015) Regional trends and controlling factors of fatal landslides in Latin America and the Caribbean. *Nat Hazards Earth Syst Sci* 15(8):1821–1833. <https://doi.org/10.5194/nhess-15-1821-2015>
- Sirbu F, Drăguț L, Oguchi T, Hayakawa Y, Micu M (2019) Scaling land-surface variables for landslide detection. *Progress Earth Planet Sci* 6(1):1–13. <https://doi.org/10.1186/s40645-019-0290-1>
- UNISDR (2018) UNISDR annual report 2017. UNISDR, Geneva. https://www.unisdr.org/files/58158_unisdr2017annualreport.pdf. Accessed 12 Nov 2019.

- USGS (2004) Landslide Types and Processes. Highway Research Board Special Report. U.S. Department of the Interior, U.S. Geological Survey. <https://pubs.usgs.gov/fs/2004/3072/pdf/fs2004-3072.pdf>. Accessed 21 Nov 2019.
- van Dessel W, van Rompaey A, Szilassi P (2011) Sensitivity analysis of logistic regression parameterization for land use and land cover probability estimation. *Int J Geogr Inf Sci* 25(3):489–508. <https://doi.org/10.1080/13658810903194256>
- van Lindert P (2016) Rethinking urban development in Latin America: a review of changing paradigms and policies. *Habitat Int* 54:253–264. <https://doi.org/10.1016/j.habitatint.2015.11.017>
- Wang Y, Feng L, Li S, Ren F, Du Q (2020) A hybrid model considering spatial heterogeneity for landslide susceptibility mapping in Zhejiang Province, China. *Catena* 188(July 2019):104425. <https://doi.org/10.1016/j.catena.2019.104425>
- Williams R (2019) Ordinal independent variables. Notre Dame. <https://www3.nd.edu/~rwilliam/xsoc73994/OrdinalIndependent.pdf>. Accessed 21 Nov 2019.
- Wubalem A (2020) Modeling of landslide susceptibility in a part of Abay Basin, northwestern Ethiopia. *Open Geosciences* 12(1):1440–1467. <https://doi.org/10.1515/geo-2020-0206>
- Zhang L, Ray H, Priestley J, Tan S (2020) A descriptive study of variable discretization and cost-sensitive logistic regression on imbalanced credit data. *J Appl Stat* 47(3):568–581. <https://doi.org/10.1080/02664763.2019.1643829>

Publisher's Note

Springer Nature remains neutral with regard to jurisdictional claims in published maps and institutional affiliations.

Submit your manuscript to a SpringerOpen[®] journal and benefit from:

- ▶ Convenient online submission
- ▶ Rigorous peer review
- ▶ Open access: articles freely available online
- ▶ High visibility within the field
- ▶ Retaining the copyright to your article

Submit your next manuscript at ▶ [springeropen.com](https://www.springeropen.com)
